

AD-A188 417

DETECTION PERFORMANCE OF NORMALIZER FOR MULTIPLE  
SIGNALS SUBJECT TO PART I (U) NAVAL UNDERWATER SYSTEMS  
CENTER NEW LONDON CT NEW LONDON LAB A H NUTTALL

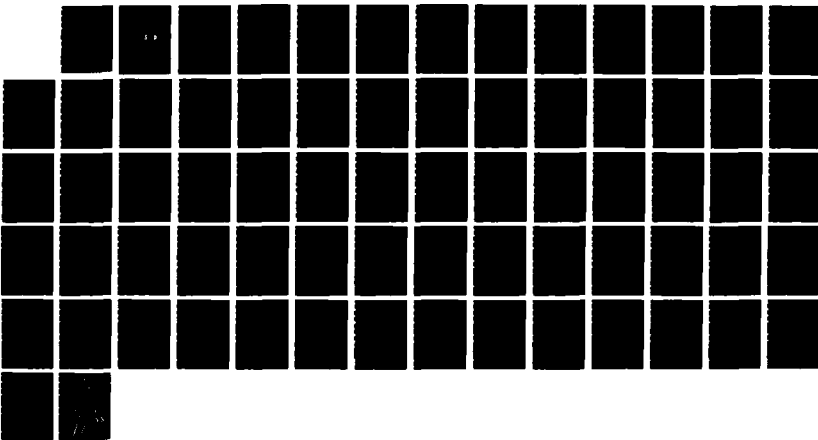
1/1

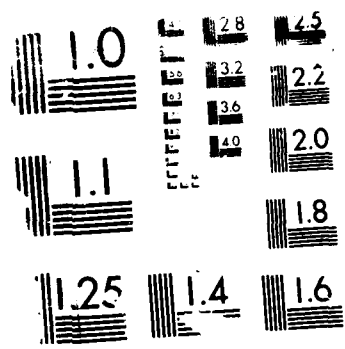
UNCLASSIFIED

01 OCT 87 NUSC-TR-8133

F/G 17/6

NL





RESOLUTION TEST CHART

2

NUSC Technical Report 8133  
1 October 1987

DTIC FILE COPY

# Detection Performance of Normalizer for Multiple Signals Subject to Partially Correlated Fading With Chi-Squared Statistics

AD-A188 417

Albert H. Nuttall  
Surface ASW Directorate

DTIC  
ELECTE  
DEC 15 1987  
S D  
C&D



**Naval Underwater Systems Center**  
Newport, Rhode Island / New London, Connecticut

Approved for public release; distribution is unlimited.

87 12 9 024

Preface

This research was conducted under NUSC Project No. A75205, Subproject No. ZR0000101, "Applications of Statistical Communication Theory to Acoustic Signal Processing," Principal Investigator, Dr. Albert H. Nuttall (Code 304). This technical report was prepared with funds provided by the NUSC In-House Independent Research and Independent Exploratory Development Program, sponsored by the Chief of Naval Research.

The Technical Reviewer for this report was Dr. G. C. Carter (Code 3314).

Reviewed and Approved:

A handwritten signature in dark ink, appearing to read 'W. A. Von Winkle', is written over the printed name.

W. A. Von Winkle

Associate Technical Director for Research and Technology

UNCLASSIFIED

SECURITY CLASSIFICATION OF THIS PAGE

## REPORT DOCUMENTATION PAGE

1a. REPORT SECURITY CLASSIFICATION UNCLASSIFIED			1b. RESTRICTIVE MARKINGS		
2a. SECURITY CLASSIFICATION AUTHORITY			3. DISTRIBUTION / AVAILABILITY OF REPORT Approved for public release; distribution is unlimited.		
2b. DECLASSIFICATION / DOWNGRADING SCHEDULE					
4. PERFORMING ORGANIZATION REPORT NUMBER(S) TR 8133			5. MONITORING ORGANIZATION REPORT NUMBER(S)		
6a. NAME OF PERFORMING ORGANIZATION Naval Underwater Systems Center		6b. OFFICE SYMBOL (If applicable) Code 304		7a. NAME OF MONITORING ORGANIZATION	
6c. ADDRESS (City, State, and ZIP Code) New London Laboratory New London, CT 06320			7b. ADDRESS (City, State, and ZIP Code)		
8a. NAME OF FUNDING / SPONSORING ORGANIZATION		8b. OFFICE SYMBOL (If applicable)		9. PROCUREMENT INSTRUMENT IDENTIFICATION NUMBER	
8c. ADDRESS (City, State, and ZIP Code)			10. SOURCE OF FUNDING NUMBERS		
			PROGRAM ELEMENT NO.	PROJECT NO.	TASK NO.
			WORK UNIT ACCESSION NO.		
11. TITLE (Include Security Classification) DETECTION PERFORMANCE OF NORMALIZER FOR MULTIPLE SIGNALS SUBJECT TO PARTIALLY CORRELATED FADING WITH CHI-SQUARED STATISTICS					
12. PERSONAL AUTHOR(S) Albert H. Nuttall					
13a. TYPE OF REPORT		13b. TIME COVERED FROM TO		14. DATE OF REPORT (Year, Month, Day) 1987 October 1	
16. SUPPLEMENTARY NOTATION					
17. COSATI CODES			18. SUBJECT TERMS (Continue on reverse if necessary and identify by block number)		
FIELD	GROUP	SUB-GROUP			
			Normalizer Correlated Fading		
			False Alarm Probability Chi-squared Fading		
			Detection Probability Multiple Pulses		
19. ABSTRACT (Continue on reverse if necessary and identify by block number)					
<p>The false alarm and detection probabilities for a multi-pulse signal subject to partially correlated fading, in the presence of Gaussian noise of unknown level, are derived in closed form. The number K of signal pulses, as well as the number L of noise-only pulses used to estimate the noise background power level, are arbitrary. The power-fading is characterized by a chi-squared distribution with 2m degrees of freedom and a normalized set of covariance coefficients, for all of which can be selected arbitrarily, in order to match an experimental realization or an actual measured situation. The performance capability of this processor depends additionally on the received signal-to-noise ratio.</p> <p>This study is an extension of NUSC Technical Report 7707, to cover the case of a nonconstant threshold. Comparisons of this normalizer with the earlier results (for <math>L = \infty</math>) enable a quantitative evaluation of the losses incurred by lack of —/over</p>					
20. DISTRIBUTION / AVAILABILITY OF ABSTRACT <input checked="" type="checkbox"/> UNCLASSIFIED/UNLIMITED <input type="checkbox"/> SAME AS RPT. <input type="checkbox"/> DTIC USERS			21. ABSTRACT SECURITY CLASSIFICATION UNCLASSIFIED		
22a. NAME OF RESPONSIBLE INDIVIDUAL Albert H. Nuttall			22b. TELEPHONE (Include Area Code) (203) 440-4618		22c. OFFICE SYMBOL Code 304

UNCLASSIFIED

SECURITY CLASSIFICATION OF THIS PAGE

## 18. SUBJECT TERMS (Cont'd.)

Unknown Noise Level  
 Constant False Alarm Rate  
 Operating Characteristics

## 19. ABSTRACT (Cont'd.)

knowledge of the noise level. The important capability of constant false alarm rate is achieved by this normalizer. ←

Plots of the detection probability vs false alarm probability are furnished for a variety of typical choices of the various parameters; however, the multitude of parameters and cases precludes a comprehensive all-encompassing compilation of numerical results. Accordingly, a general program in BASIC is listed, whereby additional results of interest to a particular user can be easily obtained, once numerical values are assigned to all the parameters.

ACCESSION FOR	
NTIS GRA&I	<input checked="" type="checkbox"/>
DTIC TAB	<input type="checkbox"/>
Unannounced	<input type="checkbox"/>
Justification	
By	
Distribution /	
Availability Codes	
DIST	Availability Codes
A-1	



UNCLASSIFIED

SECURITY CLASSIFICATION OF THIS PAGE

## TABLE OF CONTENTS

	Page
LIST OF ILLUSTRATIONS . . . . .	ii
LIST OF TABLES . . . . .	iii
LIST OF SYMBOLS . . . . .	iii
INTRODUCTION . . . . .	1
PROBLEM DEFINITION . . . . .	2
NORMALIZER PROBABILITIES . . . . .	4
Definitions of Parameters . . . . .	4
Probabilities for Known Noise Level . . . . .	5
Normalizer Ratio . . . . .	6
Normalizer Distributions . . . . .	8
Comparison With Earlier Results . . . . .	11
Special Cases . . . . .	12
Recursion for Cumulative Distribution Function . . . . .	13
Detection and False Alarm Probabilities . . . . .	15
GRAPHICAL RESULTS . . . . .	16
SUMMARY . . . . .	20
APPENDIX A - PROGRAM LISTINGS . . . . .	A-1
REFERENCES . . . . .	R-1

## LIST OF ILLUSTRATIONS

Figure		Page
1	Time-Frequency Occupancy Diagram . . . . .	2
2	ROC for $K = 1$ , $m = 1$ , $L = \infty$ . . . . .	21
3	ROC for $K = 1$ , $m = 1$ , $L = 32$ . . . . .	22
4	ROC for $K = 1$ , $m = 1$ , $L = 16$ . . . . .	23
5	ROC for $K = 1$ , $m = .5$ , $L = \infty$ . . . . .	24
6	ROC for $K = 1$ , $m = .5$ , $L = 32$ . . . . .	25
7	ROC for $K = 1$ , $m = .5$ , $L = 16$ . . . . .	26
8	ROC for $K = 2$ , $m = 1$ , $\rho = 0$ , $L = \infty$ . . . . .	27
9	ROC for $K = 2$ , $m = 1$ , $\rho = 0$ , $L = 32$ . . . . .	28
10	ROC for $K = 2$ , $m = 1$ , $\rho = 0$ , $L = 16$ . . . . .	29
11	ROC for $K = 2$ , $m = 1$ , $\rho = .5$ , $L = \infty$ . . . . .	30
12	ROC for $K = 2$ , $m = 1$ , $\rho = .5$ , $L = 32$ . . . . .	31
13	ROC for $K = 2$ , $m = 1$ , $\rho = .5$ , $L = 16$ . . . . .	32
14	ROC for $K = 2$ , $m = .5$ , $\rho = 0$ , $L = \infty$ . . . . .	33
15	ROC for $K = 2$ , $m = .5$ , $\rho = 0$ , $L = 32$ . . . . .	34
16	ROC for $K = 2$ , $m = .5$ , $\rho = 0$ , $L = 16$ . . . . .	35
17	ROC for $K = 2$ , $m = .5$ , $\rho = .5$ , $L = \infty$ . . . . .	36
18	ROC for $K = 2$ , $m = .5$ , $\rho = .5$ , $L = 32$ . . . . .	37
19	ROC for $K = 2$ , $m = .5$ , $\rho = .5$ , $L = 16$ . . . . .	38
20	ROC for $K = 4$ , $m = 1$ , $\rho = 0$ , $L = \infty$ . . . . .	39
21	ROC for $K = 4$ , $m = 1$ , $\rho = 0$ , $L = 32$ . . . . .	40
22	ROC for $K = 4$ , $m = 1$ , $\rho = 0$ , $L = 16$ . . . . .	41
23	ROC for $K = 4$ , $m = 1$ , $\rho = .5$ , $L = \infty$ . . . . .	42
24	ROC for $K = 4$ , $m = 1$ , $\rho = .5$ , $L = 32$ . . . . .	43
25	ROC for $K = 4$ , $m = 1$ , $\rho = .5$ , $L = 16$ . . . . .	44
26	ROC for $K = 4$ , $m = .5$ , $\rho = 0$ , $L = \infty$ . . . . .	45
27	ROC for $K = 4$ , $m = .5$ , $\rho = 0$ , $L = 32$ . . . . .	46
28	ROC for $K = 4$ , $m = .5$ , $\rho = 0$ , $L = 16$ . . . . .	47
29	ROC for $K = 4$ , $m = .5$ , $\rho = .5$ , $L = \infty$ . . . . .	48
30	ROC for $K = 4$ , $m = .5$ , $\rho = .5$ , $L = 32$ . . . . .	49
31	ROC for $K = 4$ , $m = .5$ , $\rho = .5$ , $L = 16$ . . . . .	50
32	SNR for $P_0 = .9$ , $K = 1$ , $m = 1$ . . . . .	51
33	SNR for $P_0 = .9$ , $K = 2$ , $m = 1$ , $\rho = .5$ . . . . .	51



## LIST OF TABLES

Table		Page
1	Fundamental Parameters . . . . .	4
2	Auxiliary Parameters . . . . .	5
3	Identification of Variables . . . . .	11

## LIST OF SYMBOLS

K	number of signal pulses added, figure 1
L	number of noise-only pulses, figure 1
m	fading parameter, table 1
$\rho_{kj}$	normalized covariance coefficient, table 1
ROC	Receiver Operating Characteristic
SNR	Signal-to-Noise Ratio
FFT	Fast Fourier Transform
$\overline{E_1}$	average received signal energy per pulse
$N_0$	single-sided noise spectral density level (watts/Hz)
$K_e$	equivalent number of samples, table 2
N	summary parameter, table 2
$\gamma$	sum of K signal squared-envelope samples
$\sigma_n^2$	noise power
a,b	auxiliary constants, (2)
R	scaled signal-to-noise ratio, (2)
$Q_\gamma$	exceedance distribution function of $\gamma$
$\Lambda$	scaled threshold, (3)
$f_n(x)$	exceedance function, (5)

## LIST OF SYMBOLS (Cont'd)

$e_n(x)$	partial exponential, (6)
$\gamma_0$	sum of $L$ noise-only squared-envelope samples
$v$	normalizer ratio output, (9)
$\tilde{v}$	alternative normalizer ratio, (10)
$u$	threshold, (11)
$P_v$	cumulative distribution function of $v$
$f(\mathcal{F})$	characteristic function, (12)
$p(u)$	probability density function, (13)
$H_2(x)$	hypergeometric function, (25)
$P_D$	detection probability, (30)
$P_F$	false alarm probability, (31)
$\rho$	exponential correlation coefficient, (32)

DETECTION PERFORMANCE OF NORMALIZER FOR MULTIPLE SIGNALS SUBJECT  
TO PARTIALLY CORRELATED FADING WITH CHI-SQUARED STATISTICS

INTRODUCTION

In a recent study [1], the detection performance capability of a multiple-pulse system subject to correlated fading was quantitatively delineated. It was assumed there that the noise level was known, so that a threshold could be set for an arbitrarily specified false alarm probability. Then the detection probability was evaluated as a function of the threshold level, the received signal-to-noise ratio, the number  $K$  of signal pulses, and the fading statistics.

Here we will extend these earlier results to cover the case where, additionally, the noise level is unknown and must be estimated on the basis of a finite number  $L$  of noise-only samples. The same approximation technique that was presented in [1] is used to determine the detection probability of this normalizer system. The reader is referred to [1] for additional background, motivation, interpretations, and related references. For the sake of brevity, we will employ the same notation and presume that the reader has complete familiarity with the earlier material and development.

## PROBLEM DEFINITION

We will couch the problem in a particular setting, one with obvious appeal and application; however, it should be obvious how to extend this setting to a more general one, particularly in light of the arbitrary fading covariance coefficients that are allowed in the analysis.

Suppose a sequence of  $K$  tone bursts at a common center frequency are transmitted, as depicted in figure 1. Each rectangular slot symbolizes

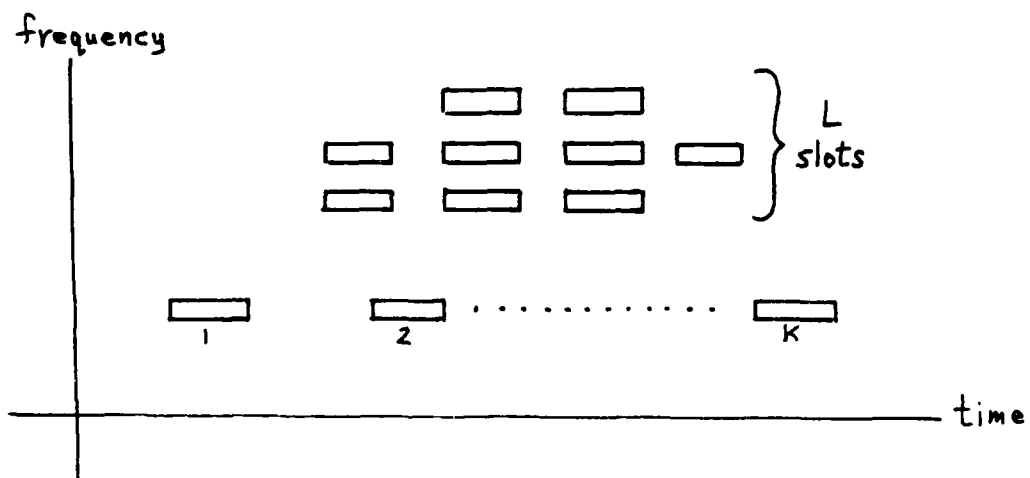


Figure 1. Time-Frequency Occupancy Diagram

a tone of duration  $T_1$  seconds and approximate frequency bandwidth  $1/T_1$  Hz. These bursts may be abutting in time or may be arbitrarily separated in time by several multiples of  $T_1$ . At the receiver,  $K$  narrowband filters of bandwidth  $1/T_1$  Hz are sampled at the times of peak signal output (if present) and their squared envelopes are summed. Depending on the time separation between pulses, the signal strength may fade considerably; the

exact amount and frequency of the fading depends on the distribution of the fading and the covariance of the fading amplitude of adjacent (as well as separated) pulses.

It is presumed that, during a single tone of duration  $T_1$  seconds, the fading is essentially constant, resulting in a constant amplitude scaling and phase shift applied to the pulse. The time separations between pulses in figure 1 are arbitrary, thereby allowing for an arbitrary degree of correlation between the fading factors applied to each pulse.

To establish a reference against which this sum of  $K$  matched filter outputs can be compared, for purposes of deciding on the presence or absence of signal, a group of  $L$  nonoverlapping noise-only slots, located arbitrarily in the time-frequency plane, are also energy-detected and summed. For very large  $L$ , this noise reference is very stable, and performance approaches that predicted by [1]. However, for moderate values of  $L$  and for small false alarm probabilities of interest, it is important to know how much degradation in performance is incurred by being forced to use this noisy reference.

An obvious implementation of the processing implied by figure 1 is to employ fast Fourier transforms. The  $L$  reference bins can then be an arbitrary collection of time and/or frequency bins. However,  $L$  cannot be so large that nonstationary and/or nonwhite noises cause their own kind of errors in noise power estimation. The tradeoff between these conflicting requirements will be assessed quantitatively in this investigation.

## NORMALIZER PROBABILITIES

## DEFINITIONS OF PARAMETERS

Very heavy reliance will be made here on the basis that was set up in [1]. Thus we have the following fundamental parameters of the detection procedure (the immediate references in tables 1 and 2 are to [1]):

$K$ , number of potential-signal pulses added, (figure 1 and A-11);

$m$ , signal fading parameter (power-scaling is chi-squared with  $2m$  degrees of freedom), (13);

$\{\rho_{kj}\}$ , normalized covariance coefficients of signal power-scalings  
 $\{q_k\}$ , (15);

$\frac{\bar{E}_1}{N_0}$ ,  $\frac{\text{average received signal energy per pulse}}{\text{single-sided received noise spectral density level}}$ , (9);

$L$ , number of noise-only pulses added.

Table 1. Fundamental Parameters

In addition, there are two very useful auxiliary parameters that found frequent use in [1]:

$$K_e, \quad K^2 / \sum_{kj=1}^K \rho_{kj} = \text{equivalent number of independent signal pulses, (10);}$$

$N, m K_e$  = a summary parameter describing the distribution of the sum of power scalings, (A-24) and (A-29).

Table 2. Auxiliary Parameters

None of the parameters,  $m, K_e, N$ , need be integer. Also,  $N$  can be larger or smaller than  $K$ , the number of signal pulses.

#### PROBABILITIES FOR KNOWN NOISE LEVEL

The probability density function of the sum  $\gamma$  [1; (A-11)] of the  $K$  signal envelope-squared samples is given by [1; (B-4)]

$$p_{\gamma}(u) = \frac{\exp(-u/a) u^{K-1}}{a^{K-N} b^N \Gamma(K)} {}_1F_1\left(N; K; u\left(\frac{1}{a} - \frac{1}{b}\right)\right) \quad \text{for } u > 0, \quad (1)$$

where [1; (A-32), (B-3), (B-7)]

$$a = 2\sigma_n^2, \quad b = 2\sigma_n^2 (1 + R), \quad R = \frac{\bar{E}_1}{N_0} \frac{K}{N}. \quad (2)$$

The exceedance distribution function  $Q_{\gamma}(u)$  of output sum  $\gamma$  is given by several alternative forms in [1; (B-9), (B-11), (B-13)]. For a fixed threshold (known noise level), the detection probability is

$$P_D = Q_Y(\mathcal{L}, R, N, K) =$$

$$= 1 - \frac{1}{(1+R)^N} \sum_{n=0}^{\infty} \frac{(N)_n}{n!} \left( \frac{R}{1+R} \right)^n \left[ 1 - E_{K-1+n}(\mathcal{L}) \right], \quad \mathcal{L} = \frac{u}{2\sigma_n^2}, \quad (3)$$

and the false alarm probability is [1; (B-10)]

$$P_F = E_{K-1}(\mathcal{L}), \quad (4)$$

where we define the exceedance distribution function

$$E_n(x) = \exp(-x) e_n(x), \quad (5)$$

and

$$e_n(x) = \sum_{j=0}^n x^j / j! \quad (6)$$

is the partial exponential [2; 6.5.11]. The results in (3) and (4) should be used for  $L = \infty$ , that is, for known noise level.

#### NORMALIZER RATIO

From this point on,  $L$  is presumed finite. Suppose a noise level estimate,  $\gamma_0$ , is obtained, based upon  $L$  independent measurements of *noise-only* bins. It is assumed that the average noise level in these  $L$  bins is the same as in the  $K$  potential-signal bins, but that this noise level is unknown. If we let



$$\gamma = \gamma(K, \bar{E}_1/N_0) \quad (7)$$

denote the sum of K signal bin outputs with average signal-to-noise ratio  $\bar{E}_1/N_0$ , then

$$\gamma_0 = \gamma(L, 0) \quad (8)$$

is the corresponding sum of L noise-only bins. Now define ratio

$$v = \frac{\gamma}{\gamma_0} = \frac{\gamma(K, \bar{E}_1/N_0)}{\gamma(L, 0)} \quad (9)$$

for sets of K and L pulses, respectively. The noise contributions to the total of K + L outputs are presumed independent of each other; however, the signal fading factors amongst the K signal outputs are correlated to an arbitrary degree. We are interested in the distribution of this normalizer ratio, v.

When signal is absent, the ratio v in (9) is independent of the absolute level of the received noise; therefore, we can expect the normalizer to achieve the important capability of constant false alarm rate. That means that a specified false alarm probability can be achieved without knowledge of the average noise power level.

The quantities  $\gamma$  and  $\gamma_0$  are the sums of K and L squared-envelope samples, respectively, and are not the averages of these sampled quantities. In terms of the sample-average quantities, we could define a slightly different normalizer ratio

$$\tilde{v} \equiv \frac{\gamma/K}{\gamma_0/L} = \frac{L}{K} v . \quad (10)$$

It then readily follows that the cumulative distribution function of random variable  $\tilde{v}$  is

$$P_{\tilde{v}}(u) = \text{Prob}(\tilde{v} < u) = \text{Prob}\left(v < \frac{K}{L} u\right) = P_v\left(\frac{K}{L} u\right) , \quad (11)$$

in terms of the cumulative distribution function of ratio  $v$  in (9). Thus, a simple scale factor change allows for consideration of the alternative ratio  $\tilde{v}$ .

When we plot the detection probability versus the false alarm probability, that is, eliminate the threshold, the same performance characteristics result for random variable  $v$  as for  $\tilde{v}$ . Accordingly, we will not use or refer to  $\tilde{v}$  or  $P_{\tilde{v}}(u)$  any further, but concentrate solely on normalizer ratio  $v$ , given by (9).

#### NORMALIZER DISTRIBUTIONS

The characteristic function of noise-only random variable  $\gamma_0$  can be found directly from [1; (A-13)] by setting  $A$  to zero and replacing  $K$  by  $L$ :

$$f_{\gamma_0}(\xi) = (1 - i\xi a)^{-L} , \quad a = 2\sigma_n^2 . \quad (12)$$

The corresponding probability density function of  $\gamma_0$  is

$$p_{\gamma_0}(u) = \frac{u^{L-1} \exp(-u/a)}{\Gamma(L) a^L} \quad \text{for } u > 0. \quad (13)$$

The exceedance distribution function is

$$Q_{\gamma_0}(u) = \text{Prob}(\gamma_0 > u) = E_{L-1}(u/a) \quad \text{for } u > 0, \quad (14)$$

in terms of the functions defined in (5) and (6).

The cumulative distribution function of ratio  $v$  in (9) is given by (since  $\gamma_0 > 0$ )

$$\begin{aligned} P_v(u) &= \text{Prob}(v < u) = \text{Prob}\left(\frac{\gamma}{\gamma_0} < u\right) = \text{Prob}(\gamma < u\gamma_0) = \\ &= \int_0^\infty dy p_\gamma(y) \int_{y/u}^\infty dx p_{\gamma_0}(x) = \int_0^\infty dy p_\gamma(y) Q_{\gamma_0}(y/u) = \\ &= \int_0^\infty dy \frac{\exp(-y/a) y^{K-1}}{a^{K-N} b^N \Gamma(K)} {}_1F_1\left(N; K; y\left(\frac{1}{a} - \frac{1}{b}\right)\right) E_{L-1}\left(\frac{y}{ua}\right) \end{aligned} \quad (15)$$

for threshold  $u > 0$ , where we used (1) and (14). We now expand  $E_{L-1}$  according to (5) and (6) and integrate term-by-term, to obtain [3; 7.621 4]

$$P_v(u) = \left(\frac{a}{b}\right)^N \left(\frac{u}{1+u}\right)^K \sum_{\ell=0}^{L-1} \frac{(K)_\ell}{\ell! (1+u)^\ell} F\left(N, K+\ell; K; \left(1 - \frac{a}{b}\right) \frac{u}{1+u}\right). \quad (16)$$

But from (2),

$$\frac{a}{b} = \frac{1}{1+R}, \quad R = \frac{\bar{E}_1}{N_0} \frac{K}{N}, \quad (17)$$

where the parameters involved are described in tables 1 and 2. Making these substitutions in (16), there follows for the cumulative distribution function of random variable  $v$ ,

$$P_v(u) = \frac{1}{(1+R)^N} \left( \frac{u}{1+u} \right)^K \sum_{\ell=0}^{L-1} \frac{(K)_\ell}{\ell! (1+u)^\ell} F\left(N, K+\ell; K; \frac{R}{1+R} \frac{u}{1+u}\right). \quad (18)$$

An alternative more useful form is obtained when we use [2; 15.3.3]:

$$P_v(u) = \left( \frac{u}{1+u} \right)^K \left( \frac{1+u}{1+u+R} \right)^N \sum_{\ell=0}^{L-1} \frac{(K)_\ell}{\ell!} \left( \frac{1+R}{1+u+R} \right)^\ell F\left(-\ell, K-N; K; \frac{R}{1+R} \frac{u}{1+u}\right) \quad (19)$$

for  $u > 0$ . This result is very attractive since the negative integer argument,  $-\ell$ , in the hypergeometric function causes termination of the series at  $\ell$  terms. Thus, (19) is a closed form (albeit tedious) for the cumulative distribution function of  $v$ , involving a finite number of elementary functions.

It should be noticed that the absolute noise level  $\sigma_n^2$  does not appear in (18) or (19). (The cumulative distribution function for alternative normalizer ratio  $\tilde{v}$  given by (10) can now easily be found by use of (11).)

## COMPARISON WITH EARLIER RESULTS

The result (19) for the cumulative distribution function of normalizer ratio  $\nu$ , operating in a partially correlated fading environment, is an approximation, having been based upon a characteristic function fitting procedure explained in [1; (A-24)-(A-28)]. Nevertheless, (19) is identical with the exact fading result for a related normalizer problem; namely, agreement with [4; (25)] is achieved under the following identifications:

<u>TR 4783</u>	<u>Here</u>	<u>Interpretation</u>
$\alpha$	$u$	threshold
$M$	$K$	number of signal pulses
$N$	$L$	number of noise-only pulses
$\nu + 1$	$N$	$m K_e$ , table 2
$\mu$	$R$	$\frac{\bar{E}_1}{N_0} \frac{K}{N}$ , (2)

Table 3. Identification of Variables

The identity of  $\nu + 1$  with  $N$  is made by comparing [4; (24A)] with [1; (A-29)]. The final identity of  $\mu$  with  $R$  utilizes [4; (24B)] and [1; (9)]:

$$\mu = \frac{\bar{R}_T}{\nu + 1} \rightarrow \frac{\bar{E}_T/N_0}{N} = \frac{\bar{E}_1}{N} \frac{K/N_0}{N} = R, \quad (20)$$

where the arrow indicates transferrance from [4] to [1].

The approach in [4] proceeded as follows: the detection probability for nonfading signals in all the bins depended only on the total received signal-to-noise ratio  $R_T$ . When  $R_T$  was assigned the fading probability density function [4; (24A)], the average detection probability in [4; (25)] resulted. For the special case of fading parameter  $\nu = M - 1$  there, numerous graphical results were given in [4; figures 1-36].

The current results here are more general, in that they allow for partially correlated fading (through parameter  $K_e$ ) and a more general power-fading model (with  $2m$  degrees of freedom). This means that  $N = m K_e$  here is not restricted to be equal to the number of signal pulses,  $K$ , but is arbitrary. Thus the current numerical results will significantly augment and extend those in [4]. If  $N = K$  here, then  $R = \bar{E}_1/N_0 =$  signal-to-noise ratio per pulse, and (19) reduces to [4; (15B)], for which many numerical results were given in [4; figures 1-36].

#### SPECIAL CASES

For  $m = 1$ , which corresponds to Rayleigh amplitude fading, and for  $\rho_{kj} = \delta_{kj}$ , which corresponds to uncorrelated fading, then  $K_e = K$ ,  $N = K$ , and we get from (19),

$$P_v(u) = \left( \frac{u}{1+u+R} \right)^K \sum_{\ell=0}^{L-1} \frac{\binom{K}{\ell}}{\ell!} \left( \frac{1+R}{1+u+R} \right)^\ell, \quad (21)$$

in agreement with [4; (15B)].

On the other hand, if  $R = 0$ , then (18) and (19) both reduce to

$$p_v^{(0)}(u) = \left(\frac{u}{1+u}\right)^K \sum_{\ell=0}^{L-1} \frac{{}^{(K)}\ell}{\ell! (1+u)^\ell}, \quad (22)$$

which is equal to  $1 - P_F$ , where  $P_F$  is the false alarm probability. Since noise level  $\sigma_n^2$  is not involved in (22), threshold  $u$  can be selected to realize a given  $P_F$ , once  $K$  and  $L$  have been specified. This is a quantitative verification of the expected constant false alarm rate property of the normalizer.

Finally, in the special case of one signal pulse,  $K = 1$ , and Rayleigh amplitude fading,  $m = 1$ , then  $K_e = 1$ ,  $N = 1$ ,  $R = \bar{E}_1/N_0$ , and (19) yields

$$P_v(u) = \frac{u}{1+u+R} \sum_{\ell=0}^{L-1} \left(\frac{1+R}{1+u+R}\right)^\ell = 1 - \left(\frac{1+R}{1+u+R}\right)^L. \quad (23)$$

That is,

$$1 - P_v(u) = \left(1 + \frac{u}{1+R}\right)^{-L}, \quad (24)$$

which agrees with [5; (6)] when we make the identifications (from there to here) of  $N \rightarrow L$ ,  $T/N \rightarrow u$ ,  $\gamma \rightarrow R$ .

#### RECURSION FOR CUMULATIVE DISTRIBUTION FUNCTION

Let the hypergeometric function appearing in (19) be represented as follows:

$$H_\ell(x) \equiv \frac{{}^{(K)}\ell}{\ell!} F(-\ell, K - N; K; x). \quad (25)$$

Then

$$H_0(x) = 1, \quad (26)$$

while (25) has the recursion [2; 15.2.10]

$$\ell H_\ell(x) = [K + 2\ell - 2 + (N - K + 1 - \ell)x] H_{\ell-1}(x) - (K + \ell - 2)(1 - x)H_{\ell-2}(x) \\ \text{for } \ell \geq 1, \quad (27)$$

where we define  $H_{-1}(x) = 0$ . In terms of (25), the cumulative distribution function of  $v$  in (19) becomes

$$P_v(u) = \left(\frac{u}{1+u}\right)^K \left(\frac{1+u}{1+u+R}\right)^N \sum_{\ell=0}^{L-1} \left(\frac{1+R}{1+u+R}\right)^\ell H_\ell\left(\frac{R}{1+R} \frac{u}{1+u}\right). \quad (28)$$

This form, in conjunction with recursion (27), was used for all the numerical results here, for  $L$  finite. The parameters appearing in (28) have all been explained in tables 1 and 2. The explicit dependence on the fundamental parameters is indicated below:

$$K_e = K_e(K, \{\rho_{kj}\}), \\ N = N(m, K, \{\rho_{kj}\}), \\ R = R(\bar{E}_1/N_0, m, K, \{\rho_{kj}\}). \quad (29)$$

In addition, the cumulative distribution function in (28) is a function of  $L$  and threshold  $u$ .



## DETECTION AND FALSE ALARM PROBABILITIES

The detection probability is given by

$$P_D = \text{Prob}(v > u | R > 0) = 1 - P_v(u), \quad (30)$$

where  $P_v(u)$  is available in (28). The false alarm probability is

$$P_F = \text{Prob}(v > u | R = 0) = 1 - p_v^{(0)}(u), \quad (31)$$

where  $p_v^{(0)}(u)$  is available in (22). By allowing threshold  $u$  to vary over a wide range,  $P_D$  and  $P_F$  values can be obtained and plotted against each other, resulting in the standard receiver operating characteristics; the threshold is thereby eliminated from the plotted outputs. Programs for plotting  $P_D$  vs  $P_F$ , both for  $L$  finite as well as infinite, are listed in appendix A.

## GRAPHICAL RESULTS

Due to the multitude of parameters appearing in this investigation (see tables 1 and 2), it is impossible to give a comprehensive compilation of encompassing numerical results. Considering just the covariance coefficients  $\{\rho_{kj}\}_1^K$  for the moment, complete specification requires assignment of  $K(K - 1)/2$  values to these quantities; to circumvent this difficulty, we consider numerically, here, only the very special case of exponential correlation, for which

$$\rho_{kj} = \rho^{|k-j|} \quad \text{for } 1 \leq k, j \leq K, \quad (32)$$

and look at a couple of particular values for  $\rho$ . Our approach here, of necessity, is to give some representative sample receiver operating characteristics and a general computer program in BASIC, whereby additional results can easily be obtained once the user has specified all the particular values of interest in his application. This program allows for arbitrary covariance coefficients,  $\{\rho_{kj}\}$ , and is not limited to the specific example (32).

The particular cases we will investigate are as follows:

$$\begin{aligned} K &= 1, 2, 4, \\ L &= 16, 32, \infty, \\ m &= .5, 1, \\ \rho &= 0, .5. \end{aligned} \quad (33)$$

All possible combinations of these four fundamental variables lead to 30 plots, which appear below<sup>\*</sup> in figures 2-31. (There are only 6 plots for  $K = 1$ , not 12, because the value of  $\rho$  is irrelevant for  $K = 1$ ). The curves are indexed by the per-pulse signal-to-noise ratio,  $\bar{E}_1/N_0$ , in dB. The false alarm and detection probability pairs range from (poor quality) pair (.5, .01) up to (high quality) pairs near ( $1E-10$ , .999).

The number of signal pulses,  $K$ , is limited to the low values 1, 2, 4, because these seem to be the cases of most immediate practical use. The number of noise-only samples,  $L$ , is not evaluated for  $L = 64$  because of the proximity of the results to those for  $L = \infty$ ; conversely, results are not presented for  $L = 8$ , because a severe degradation in performance occurs, that probably cannot be tolerated. The fading parameter value  $m = 1$  corresponds to Rayleigh amplitude fading (exponential power fading), while  $m = .5$  corresponds to a deeper more-damaging form of fading. The correlation coefficient  $\rho = 0$  corresponds to uncorrelated (independent) fading, while  $\rho = .5$  allows for adjacent (equispaced) pulses in figure 1 to have some degree of dependent fading.

An explanation of the initial result in figure 2 follows: for  $K = 1$ ,  $m = 1$ ,  $L = \infty$  (known noise level), the detection probability is plotted versus the false alarm probability for values of the latter between  $1E-10$  and .1. The value of the per-pulse signal-to-noise ratio,  $\bar{E}_1/N_0$  in dB, varies over the range 6, 8, 10, ... , 42, giving detection probability values covering

\* All the figures are collected together after the Summary section.

the range .01 to .999. The only difference in the accompanying pair, figures 3 and 4, is that  $L$  is reduced to 32 and 16, respectively.

The results in figures 5 through 7 correspond to the worst cases considered here. Namely, there is just one (fading) signal pulse and  $m$  is .5, which means a very deep fading medium; see [1; figure 2]. The values of signal-to-noise ratio required for  $L = 16$  in figure 7 are so large as to be physically unrealistic, except for the poorer quality region.

On the other hand, for  $K = 4$  signal pulses, Rayleigh amplitude fading ( $m = 1$ ), and uncorrelated fading ( $\rho = 0$ ), the results in figures 20 through 22 are very encouraging, being physically reasonable over the whole range of plotted values. But when  $m$  is decreased to .5, and  $\rho$  is increased to .5, the results in figures 29 through 31, still for  $K = 4$  pulses, indicate substantially increased signal-to-noise ratio requirements at the higher quality end of the performance region.

An alternative method of presenting the graphical results, which accounts for the losses incurred by not knowing the noise level, is to plot the required value of  $\bar{E}_1/N_0$  vs  $L$ , for various values of the remaining parameters and for specified performance quality in terms of  $P_F$  and  $P_D$ . Two such cases are illustrated in figures 32 and 33. They show that the cost of not knowing the noise level is not severe for the high false alarm probabilities, but is quite significant for the lower more-desirable false alarm probabilities. For example, in figure 33 for  $K = 2$  signal pulses, the signal-to-noise ratio must be about 1.5 dB larger at  $L = 10$  noise pulses than

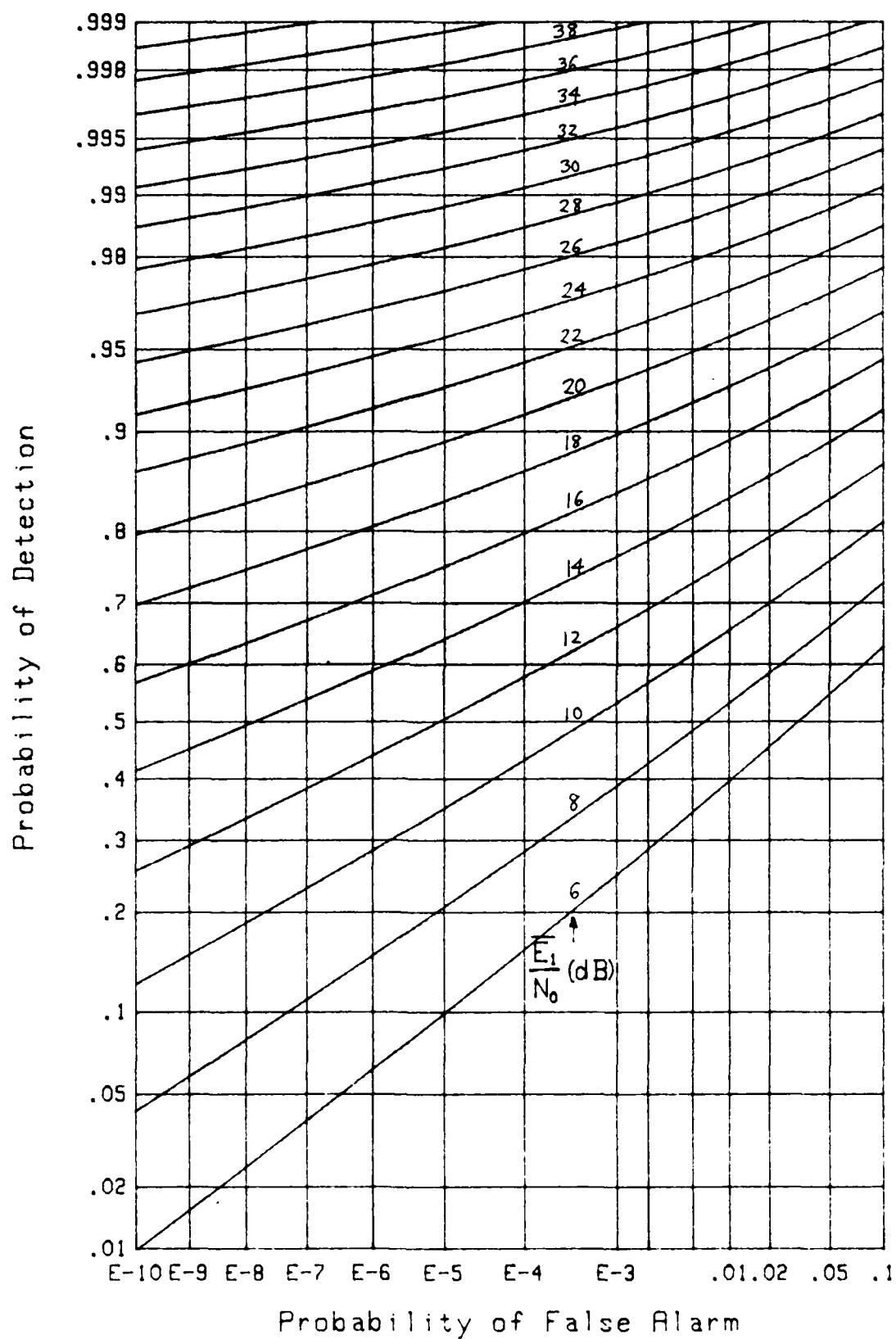
at  $L = 100$ , when  $P_F = .01$ . However, if we want to operate at  $P_F = 1E-10$ , the increased signal-to-noise ratio requirement is about 6 dB per pulse. The numbers are comparable for the  $K = 1$  results in figure 32.

The asymptotes for large  $L$  in figures 32 and 33 can be found in some cases from earlier results in [1]. For example, reference to [1; figure 8] for  $K = 2$ ,  $\rho = .5$  gives  $\bar{E}_1/N_0 \cong 16.8$  dB, while  $P_F = 1E-6$ ,  $P_D = .9$ ,  $m = 1$ . Comparison with figure 33 here reveals that the performance requirement is virtually at this level by the time that  $L = 100$ .

## SUMMARY

Although figures 32 and 33 are very informative, allowing for a ready assessment of the losses incurred by using a finite small value for  $L$ , the number of noise-only pulses, they also illustrate the voluminous compilation that would be needed for a thorough numerical investigation. For example, if: detection probabilities  $P_D$  were of interest for values .5, .9, .99, .999; number of signal pulses  $K$  for values 1, 2, ... , 10; fading parameter  $m$  for values .5, 1, 2; and fading correlation coefficient  $\rho$  for 0, .5, 1; this would require a total of  $4 \times 10 \times 3 \times 3 = 360$  figures. The approach here is instead to present some representative receiver operating characteristics, in figures 2 through 31, from which information similar to that in figures 32 and 33 can be extracted, and to list a general program for the generation of additional receiver operating characteristics for whatever cases may be of interest to the user.

Some related work on the performance of a log-normalizer subject to Weibull or log-normal inputs has been published by the author in [6]; however, no fading was allowed, and the number of signal pulses was limited to  $K = 1$ . In a different vein, the performance of an or-ing device operating on the output of an incoherent combiner of multiple pulses was analyzed in [7]. These works augment and complement the analysis conducted here.

Figure 2. ROC for  $K=1$ ,  $m=1$ ,  $L=\infty$

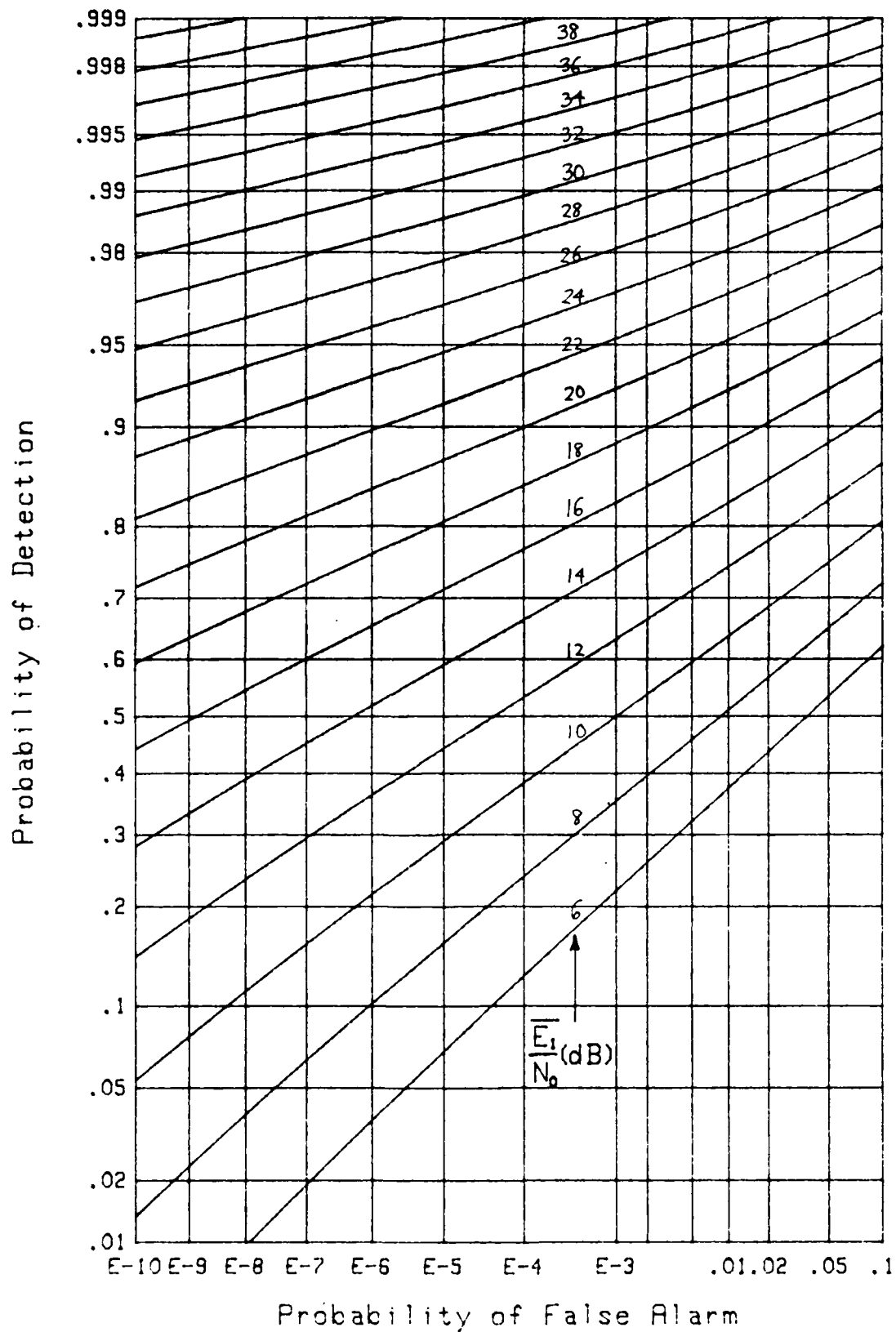


Figure 3. ROC for  $K=1$ ,  $m=1$ ,  $L=32$



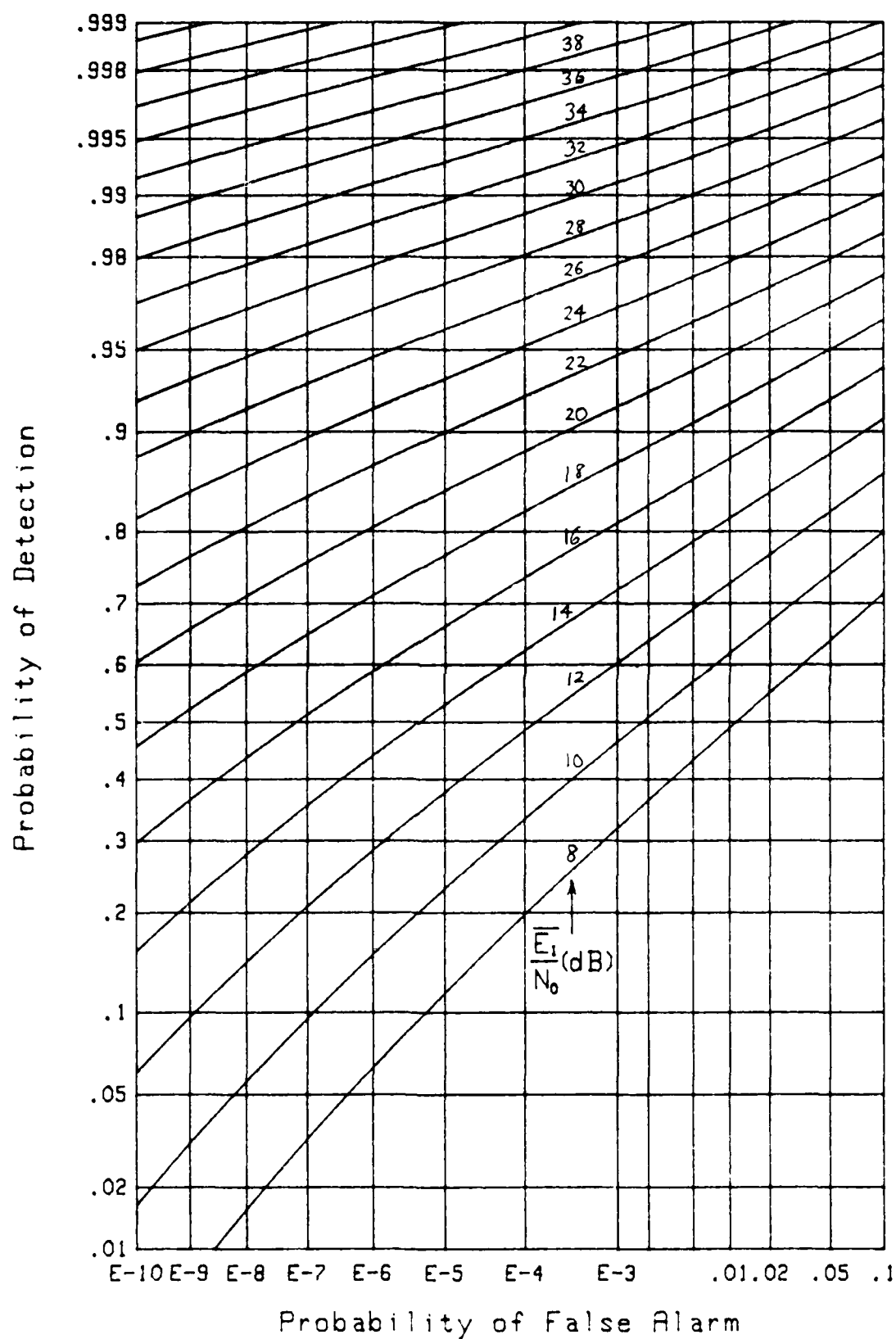
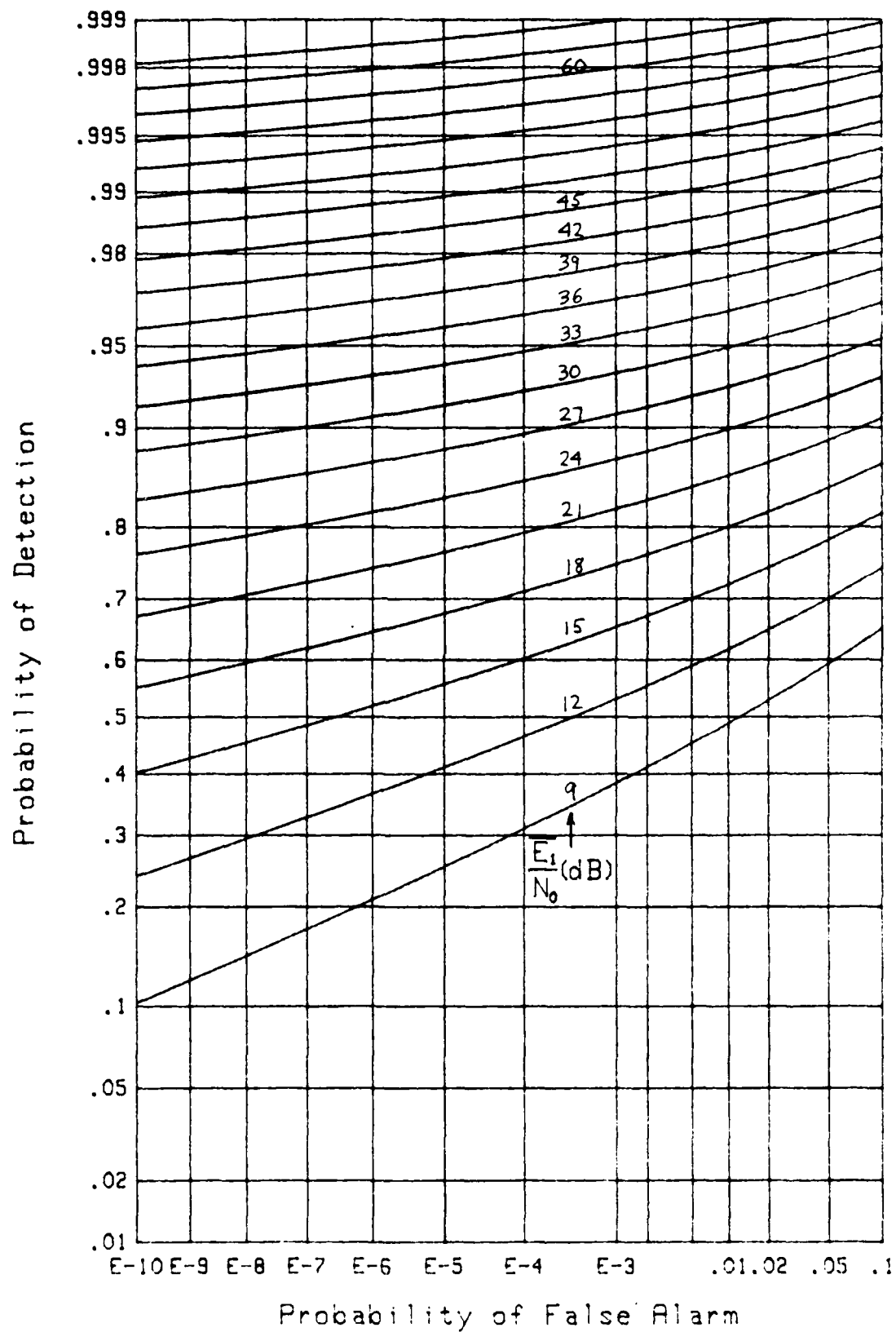
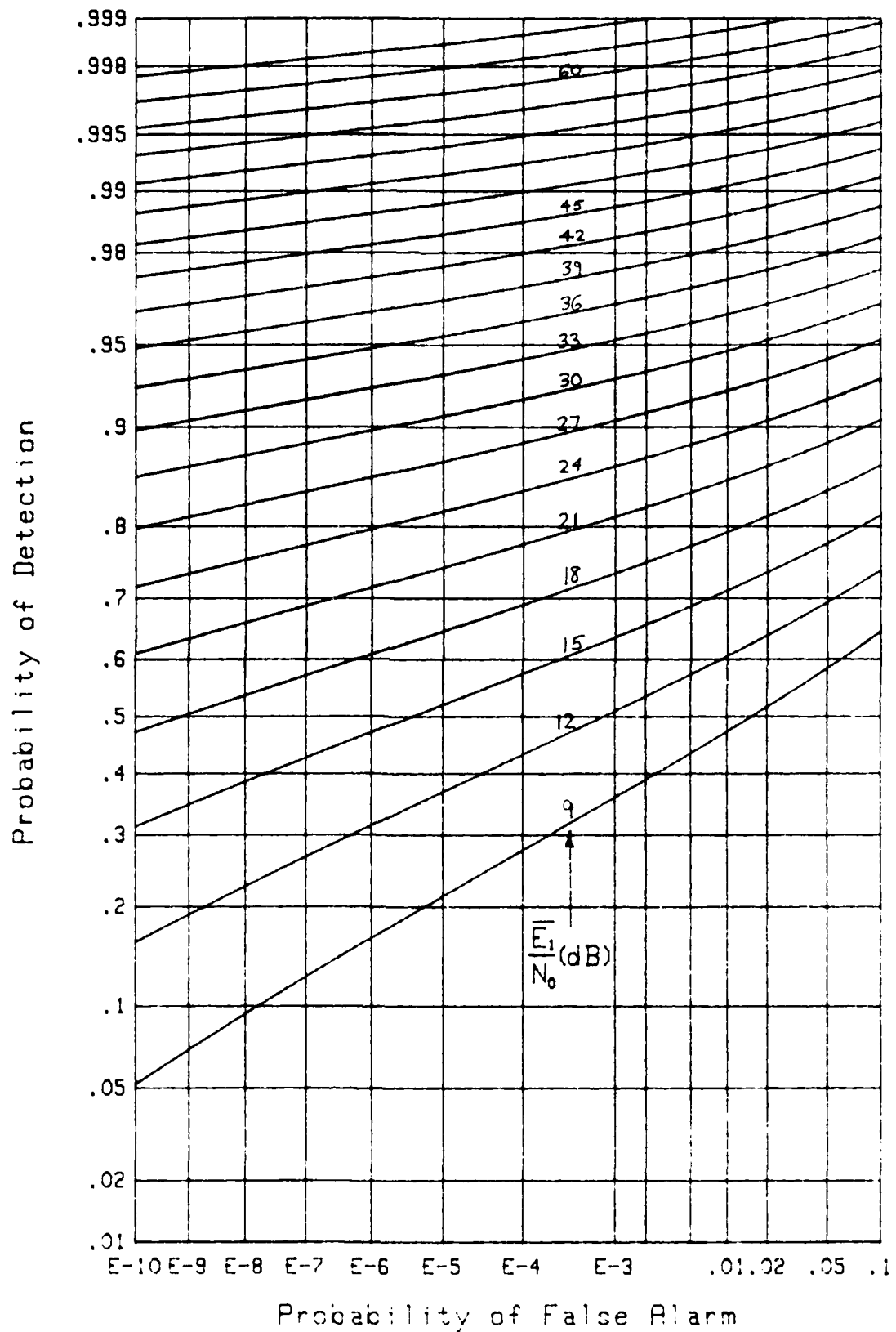


Figure 4. ROC for K=1, m=1, L=16

Figure 5. ROC for  $K=1$ ,  $m=.5$ ,  $L=\infty$

Figure 6. ROC for  $K=1$ ,  $m=.5$ ,  $L=32$

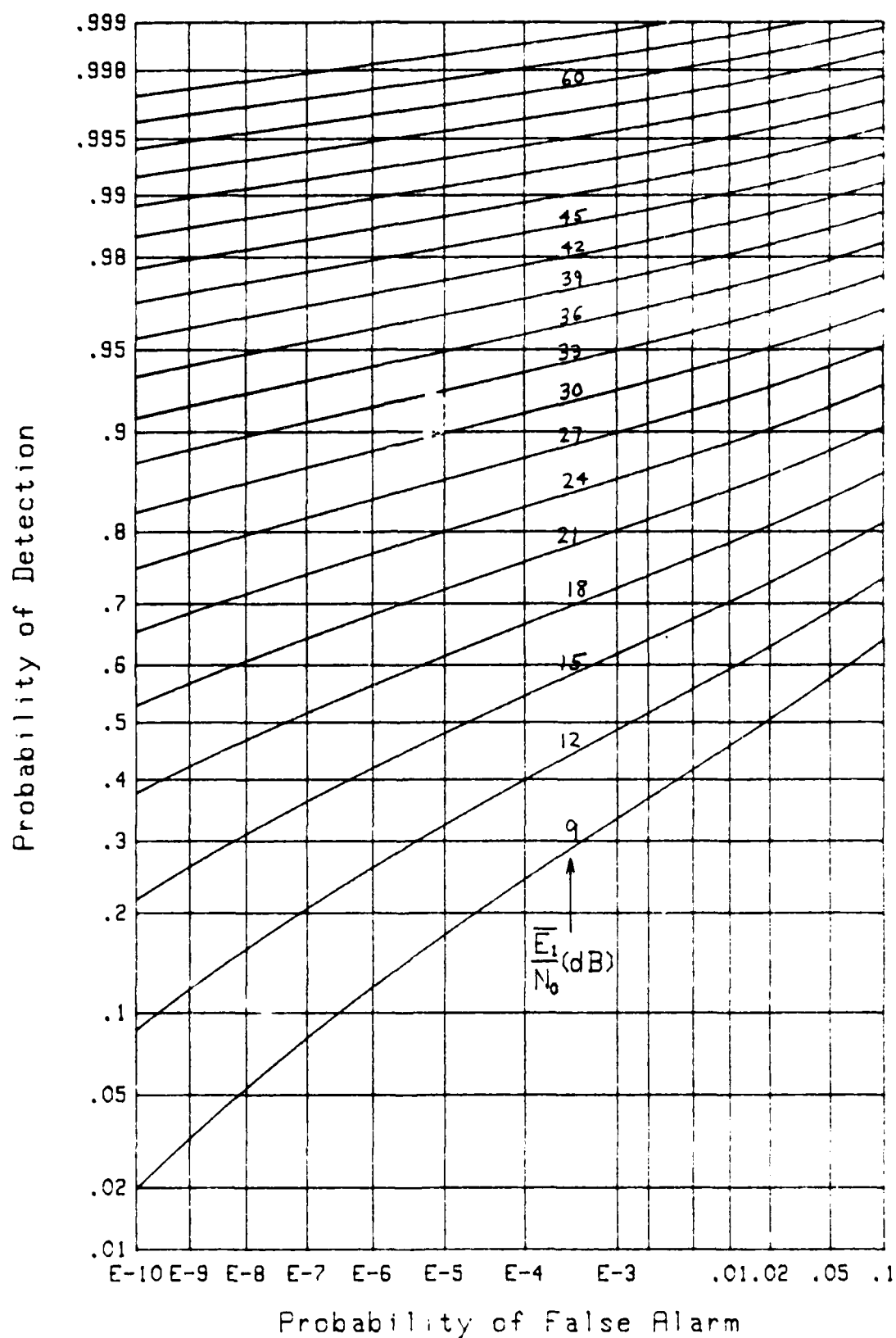
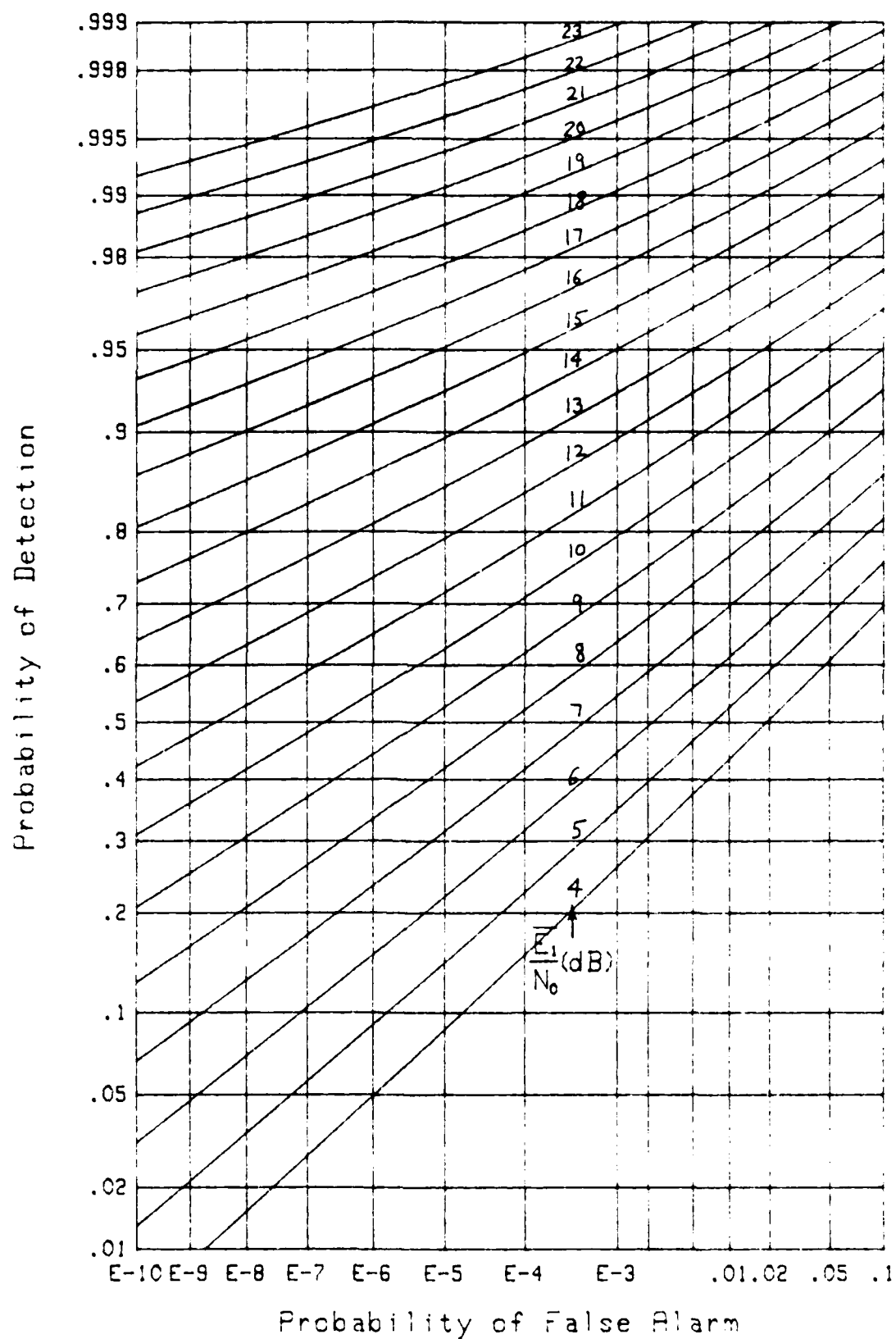
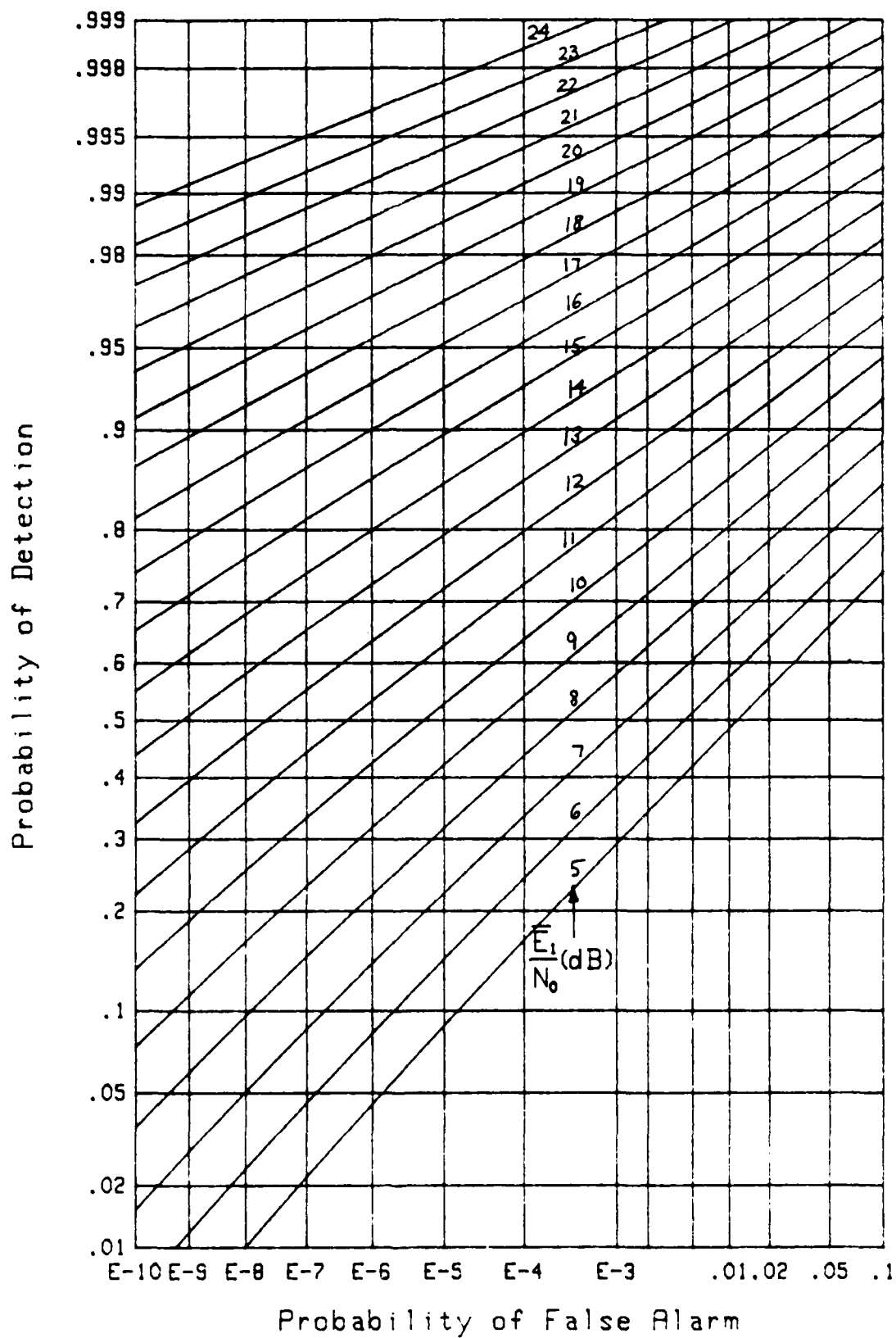
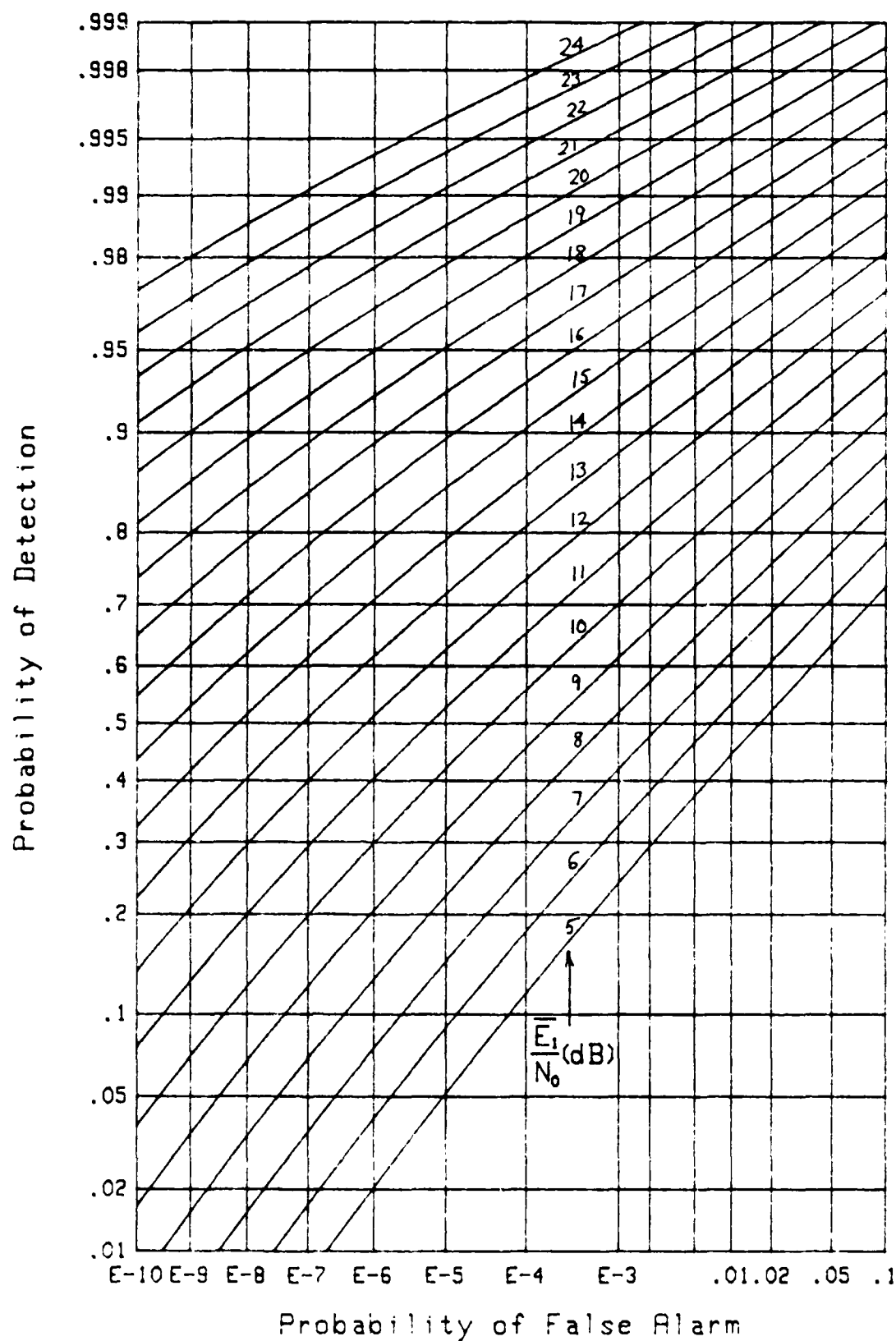
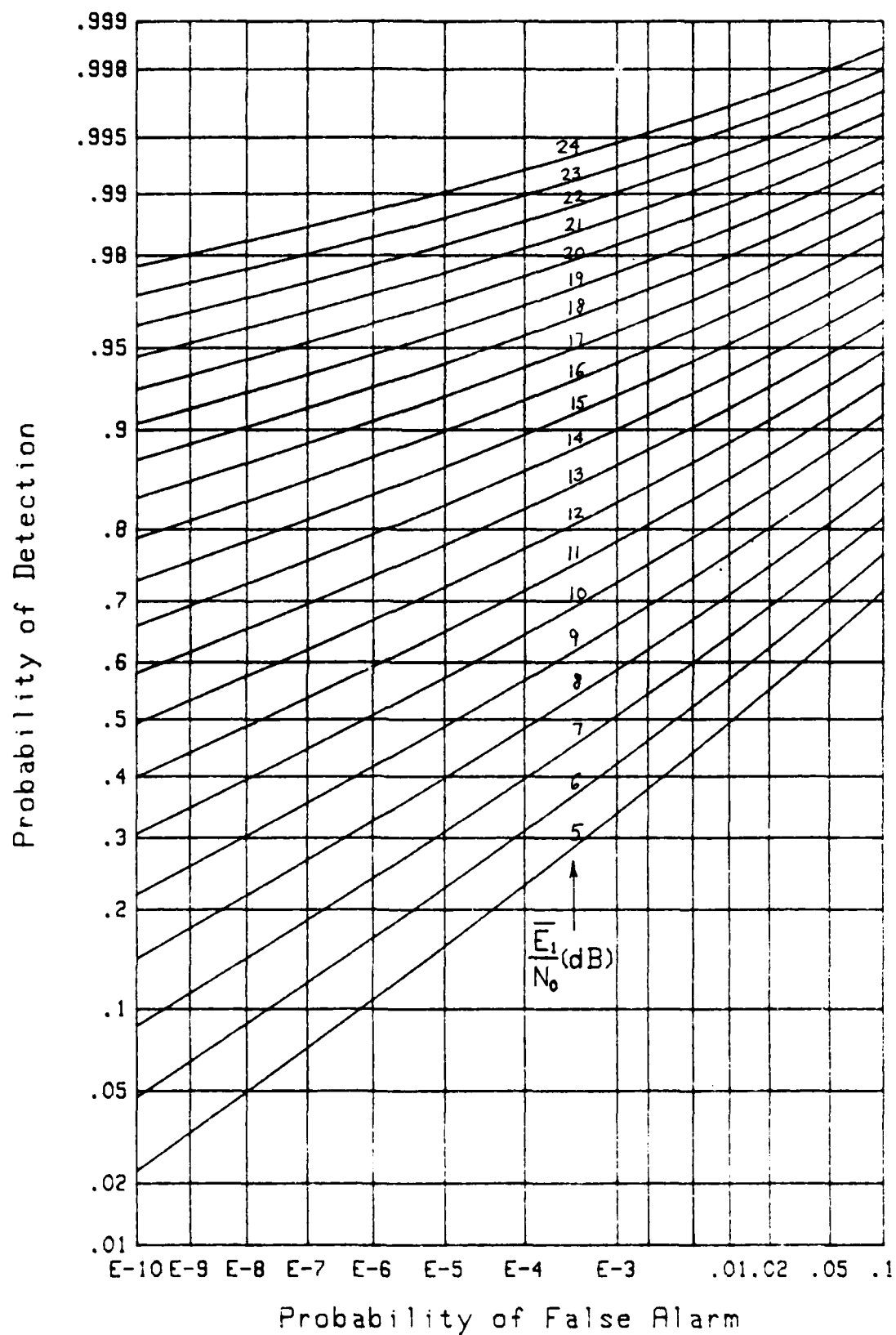


Figure 7. ROC for K=1, m=.5, L=16

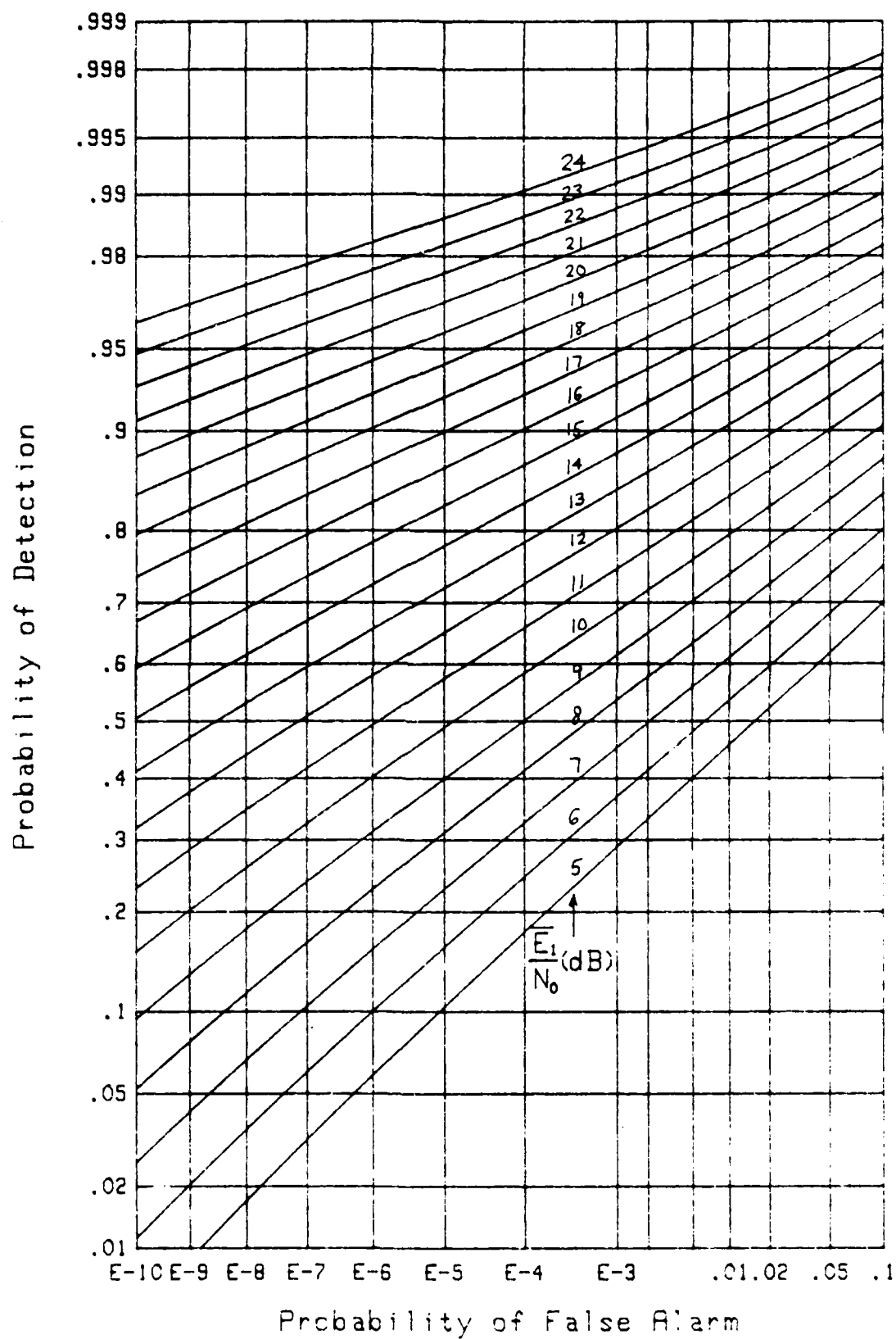
Figure 8. ROC for  $K=2$ ,  $m=1$ ,  $\rho=0$ ,  $L=\infty$

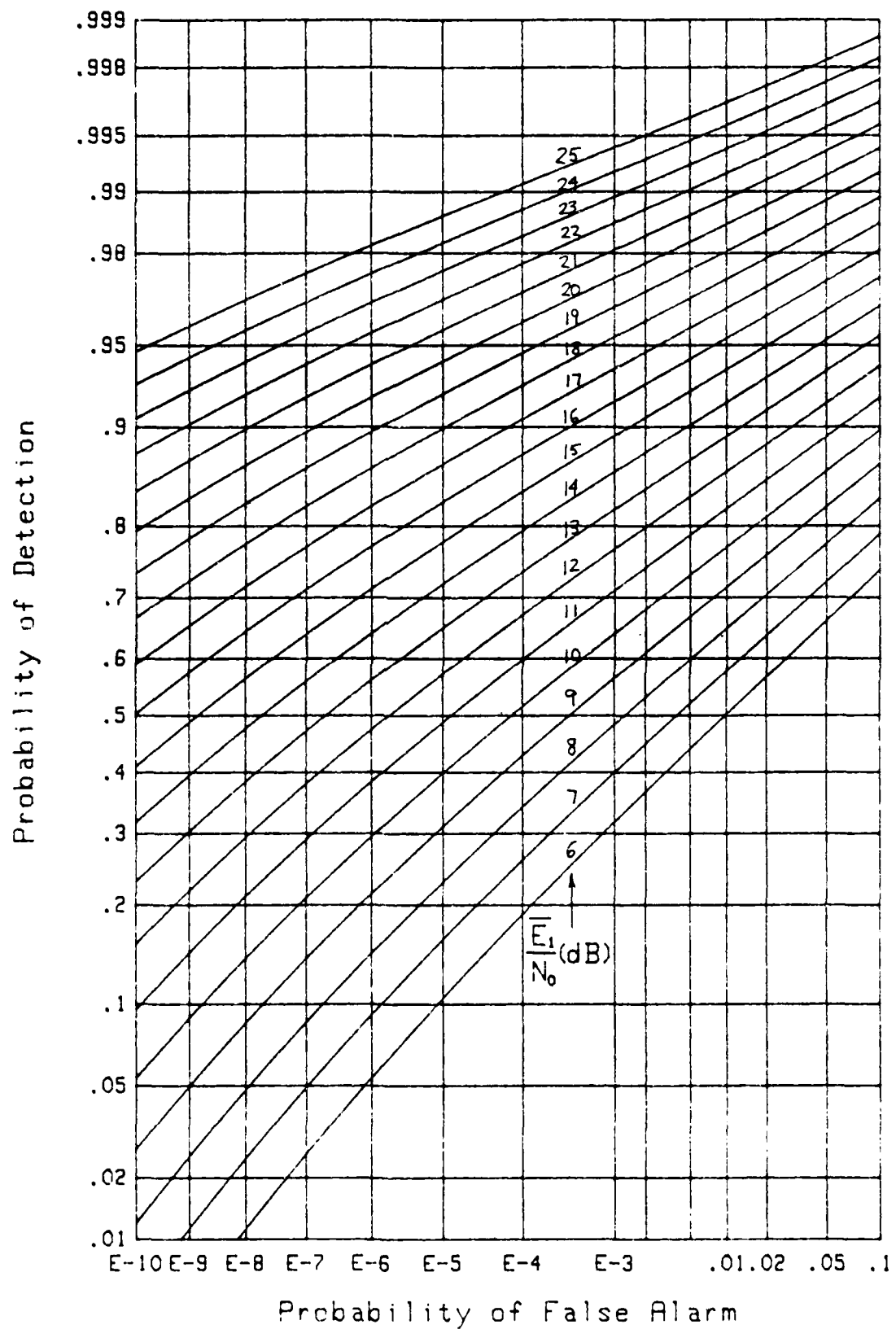
Figure 9. ROC for  $K=2$ ,  $m=1$ ,  $\rho=0$ ,  $L=32$

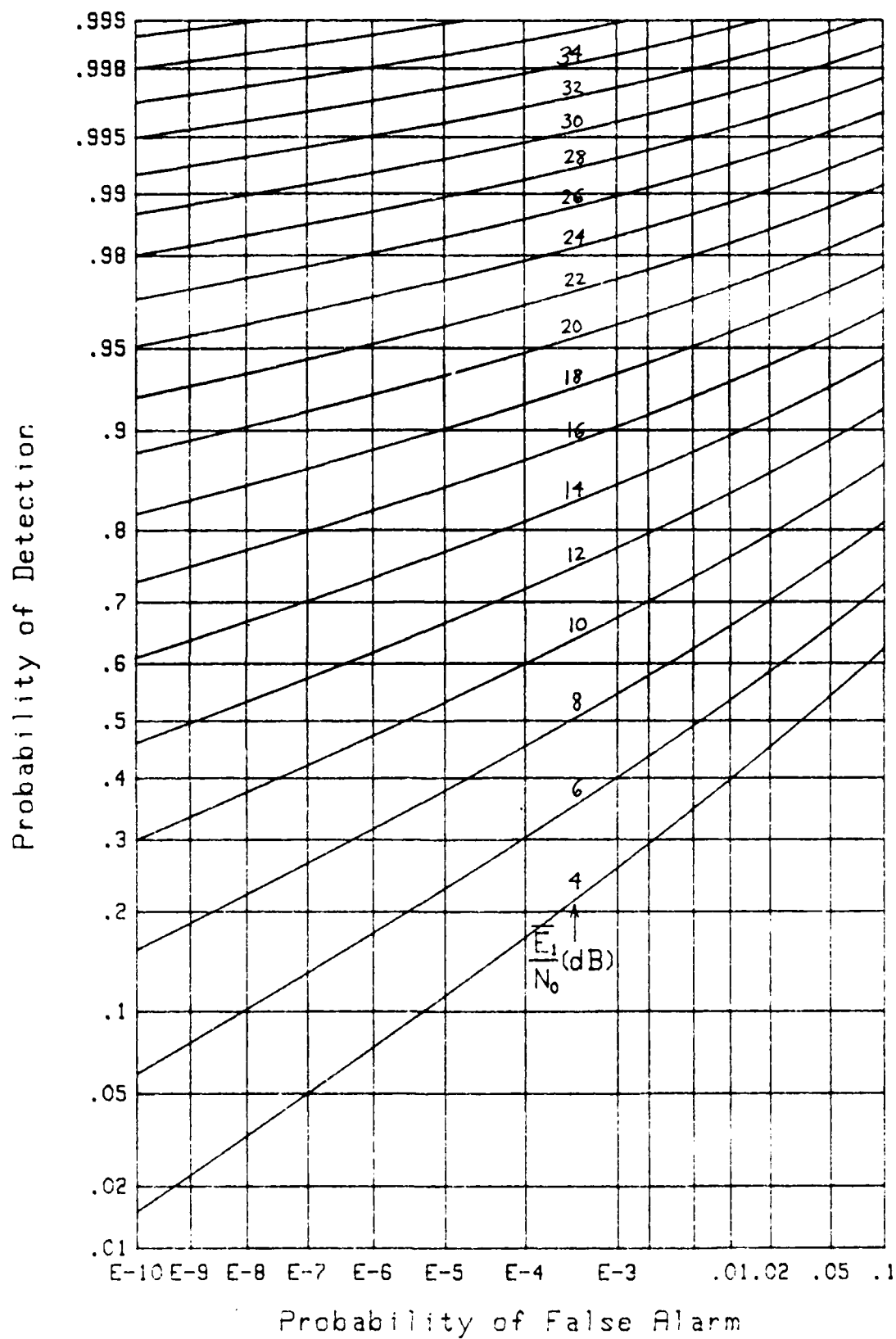
Figure 10. ROC for  $K=2$ ,  $m=1$ ,  $p=0$ ,  $L=16$

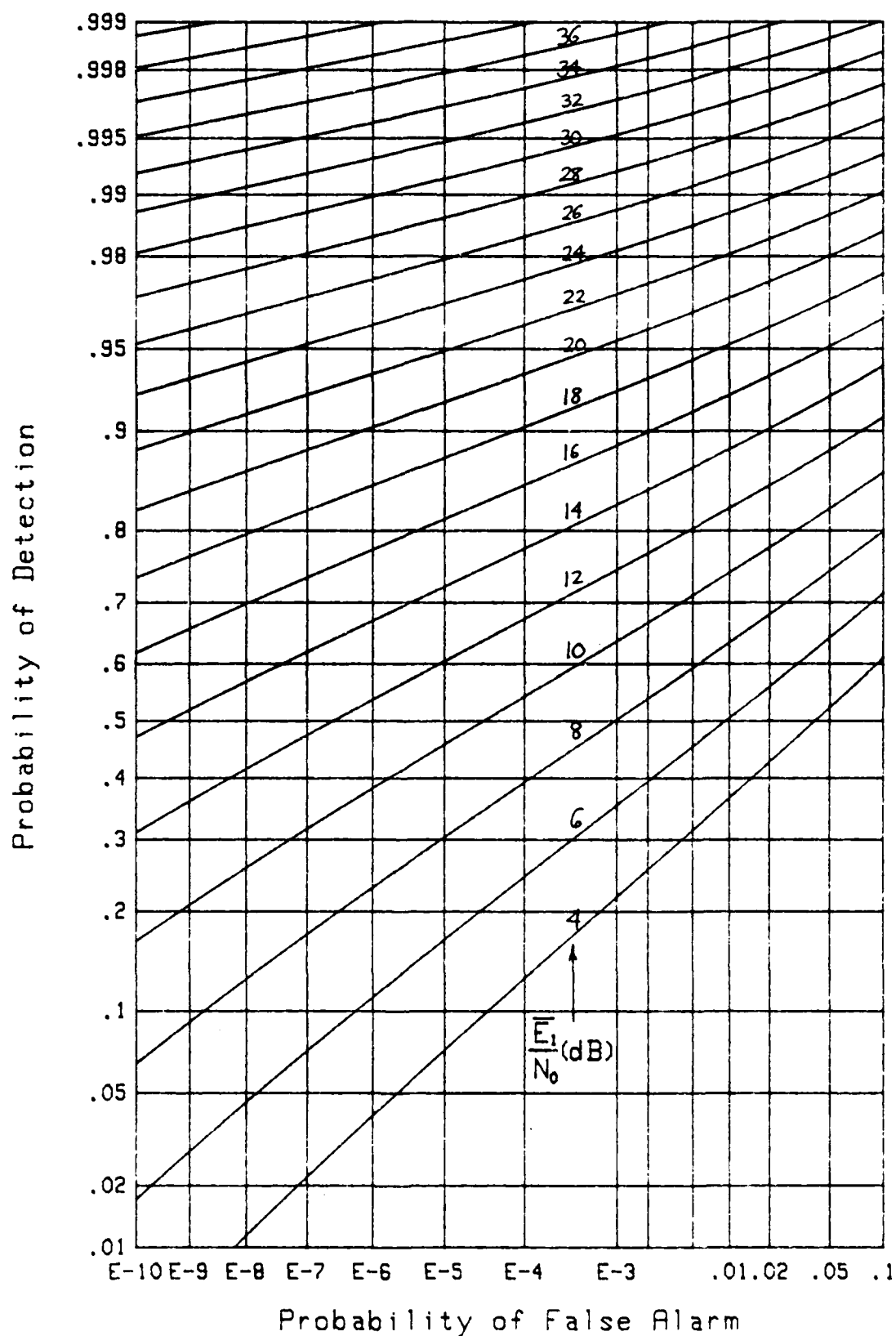
Figure 11. ROC for  $K=2$ ,  $m=1$ ,  $\rho=.5$ ,  $L=\infty$

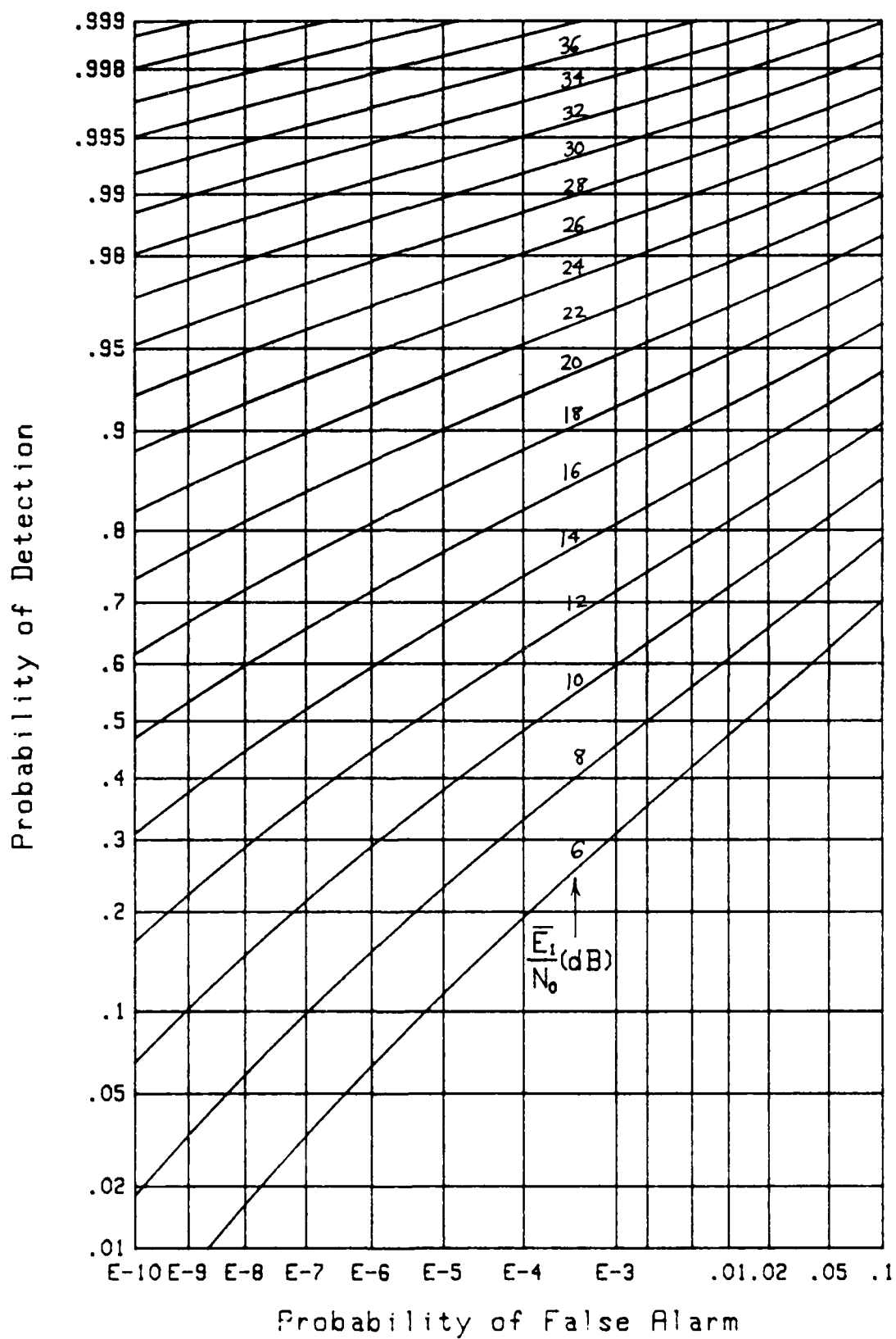


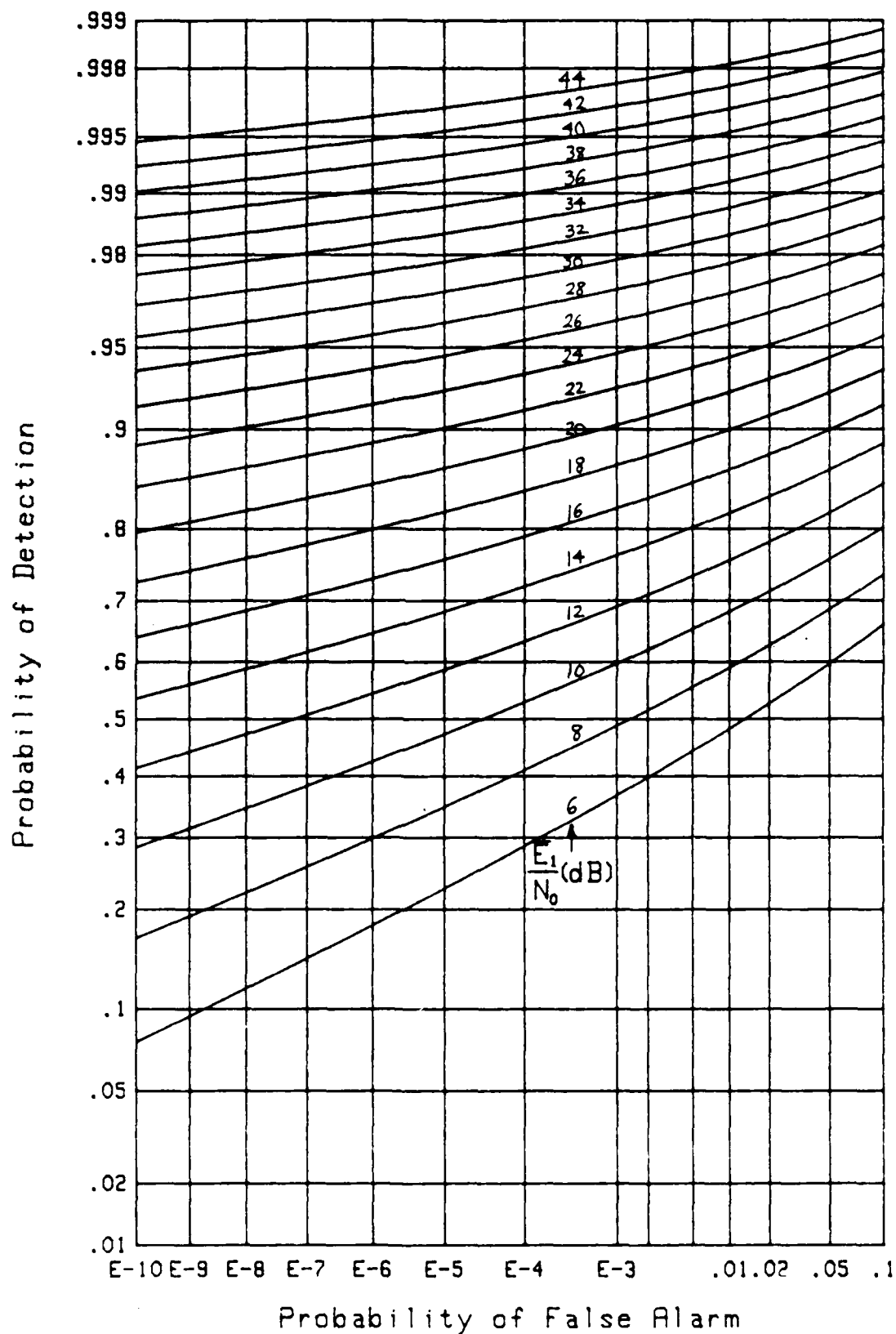
Figure 12. ROC for  $K=2$ ,  $m=1$ ,  $\rho=.5$ ,  $L=32$

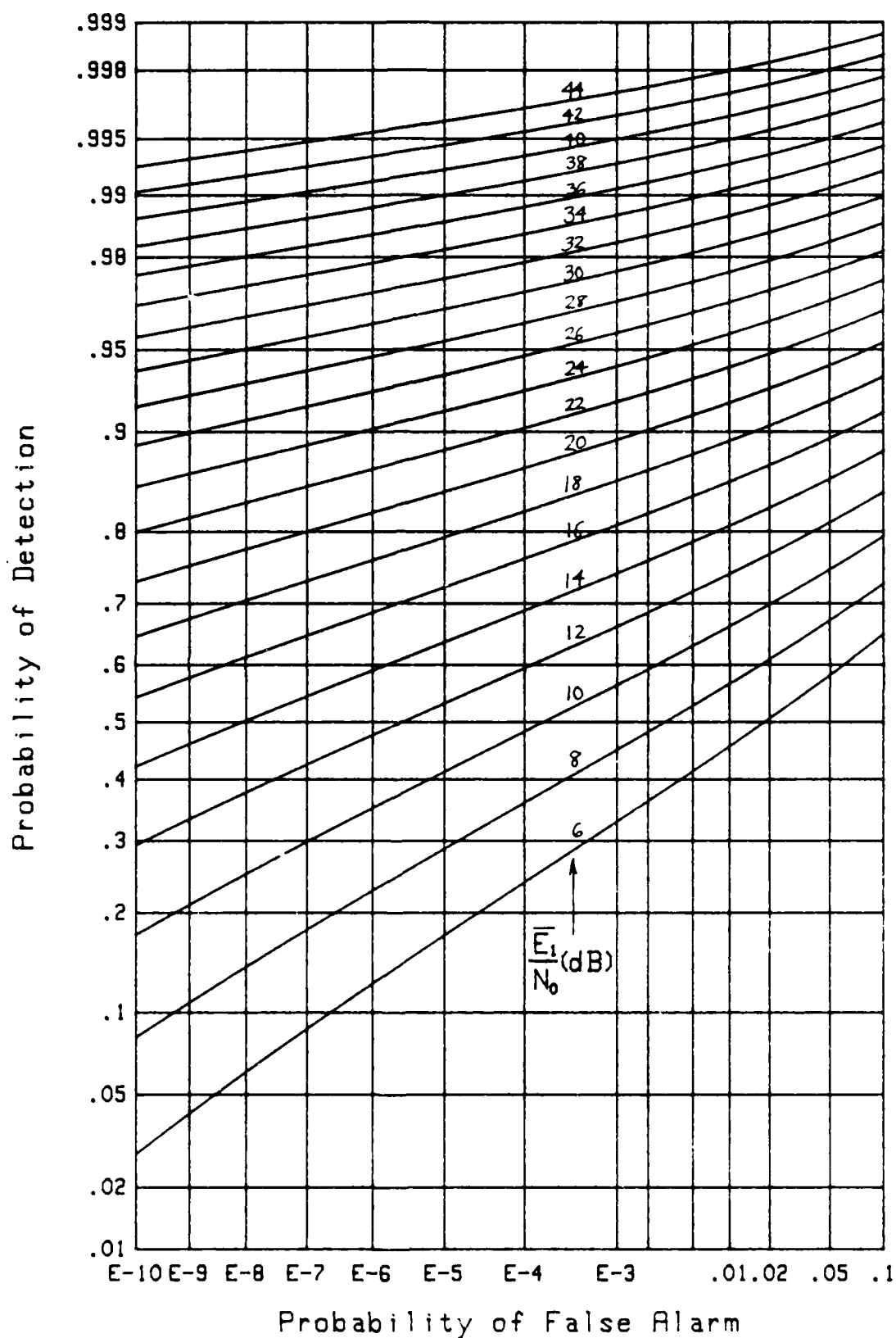
Figure 13. ROC for  $K=2$ ,  $m=1$ ,  $\rho=.5$ ,  $L=16$

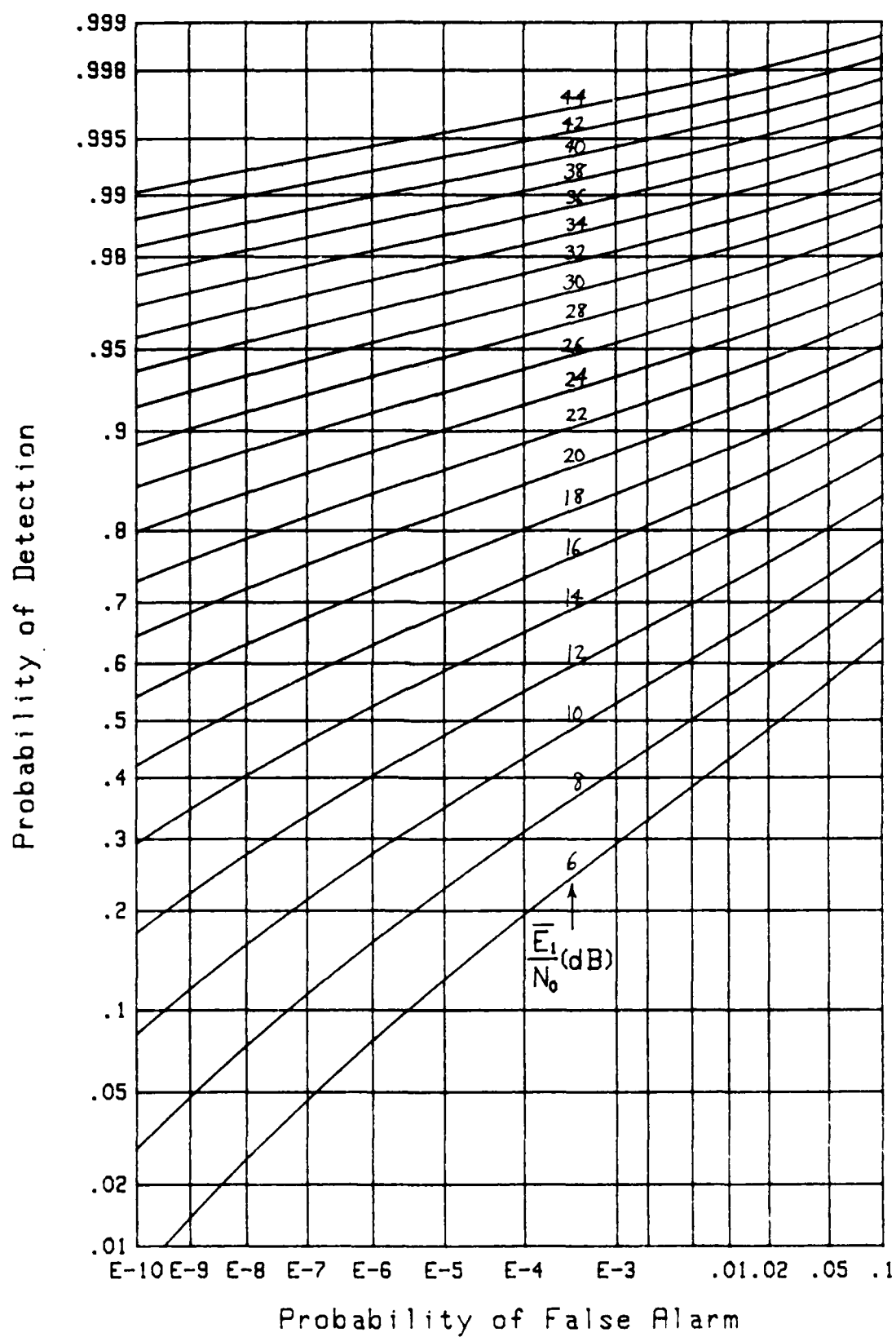
Figure 14. ROC for  $K=2$ ,  $m=.5$ ,  $\rho=0$ ,  $L=\infty$

Figure 15. ROC for  $K=2$ ,  $m=.5$ ,  $\rho=0$ ,  $L=32$

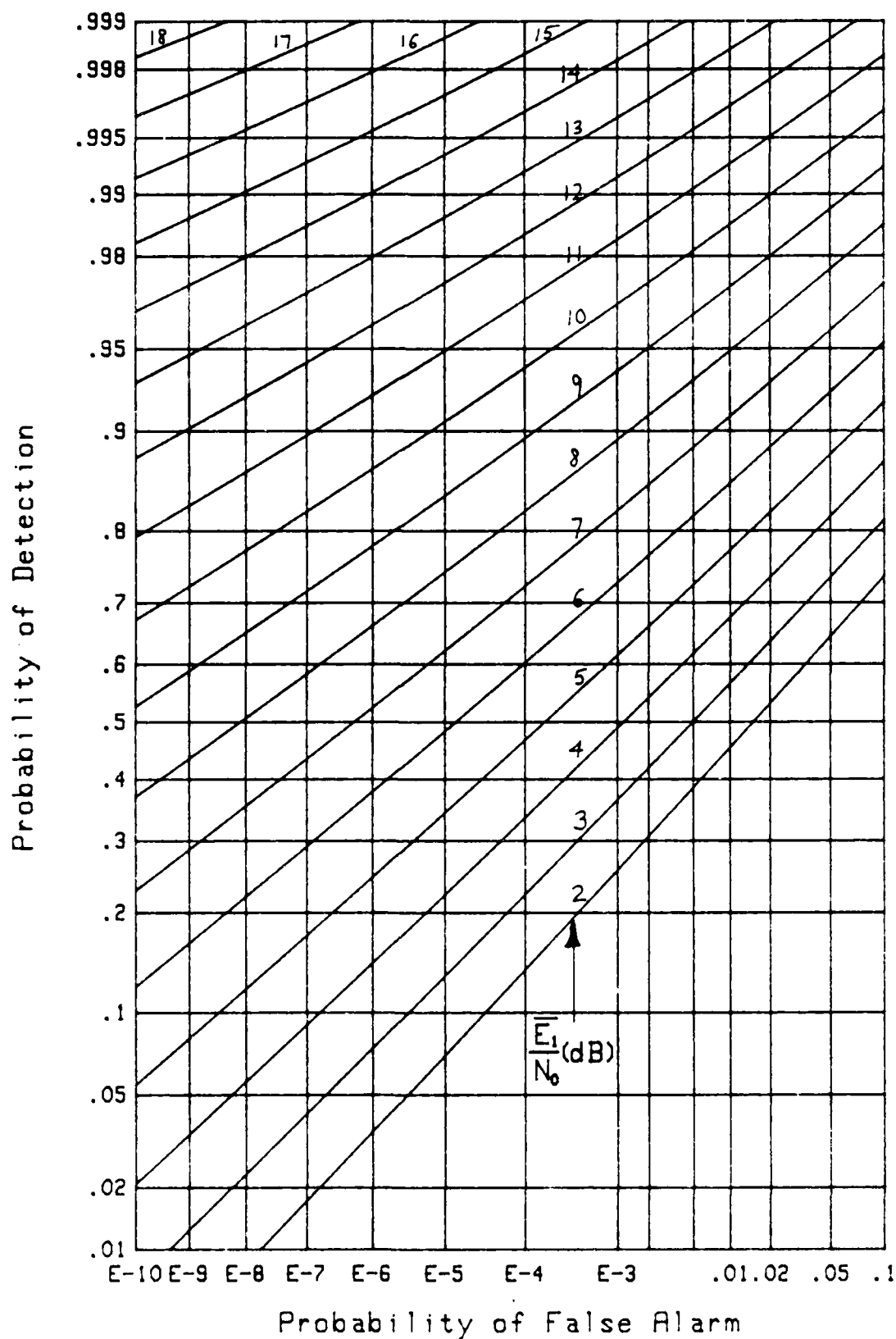
Figure 16. ROC for  $K=2$ ,  $m=.5$ ,  $\rho=0$ ,  $L=16$

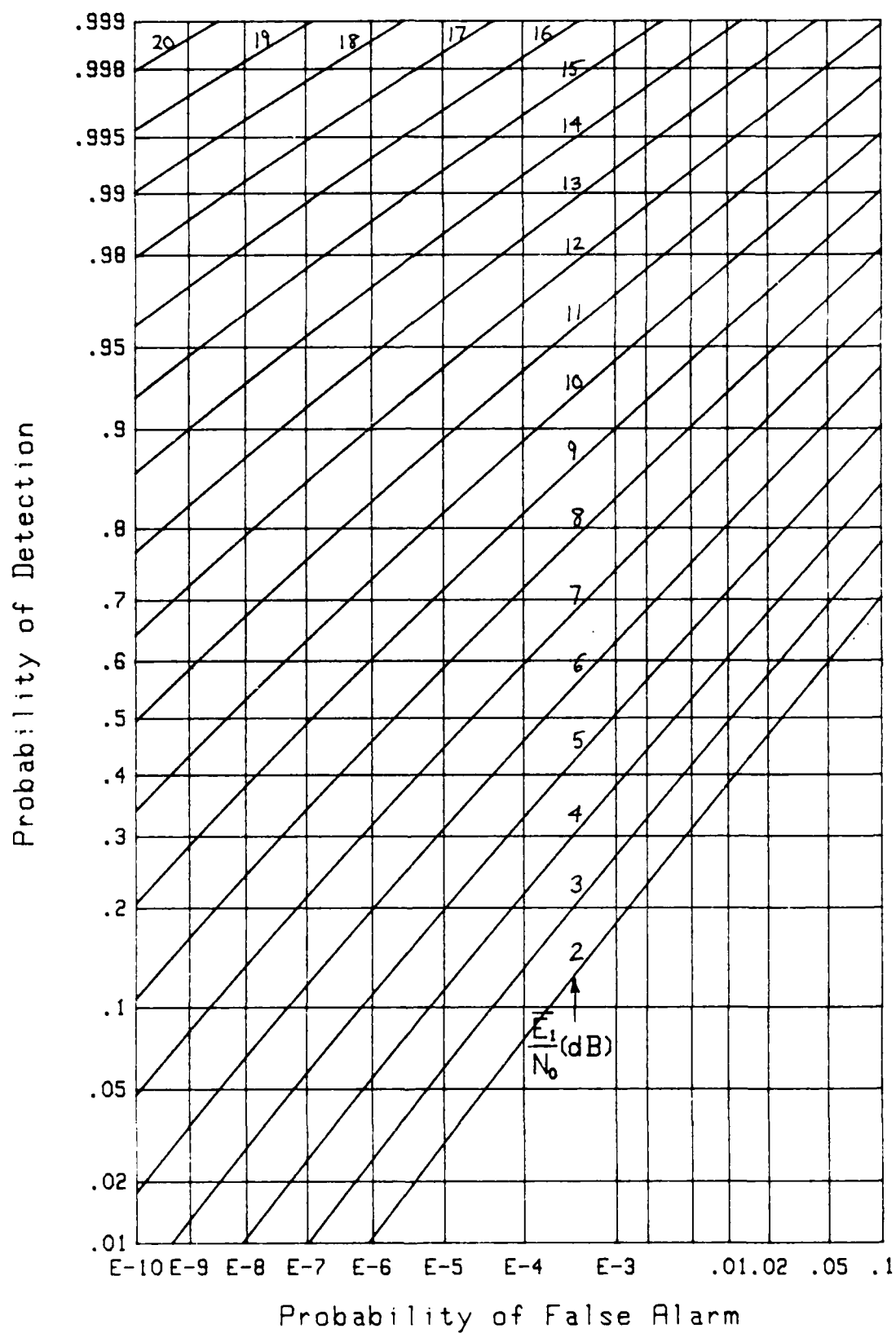
Figure 17. ROC for  $K=2$ ,  $m=.5$ ,  $\rho=.5$ ,  $L=\infty$

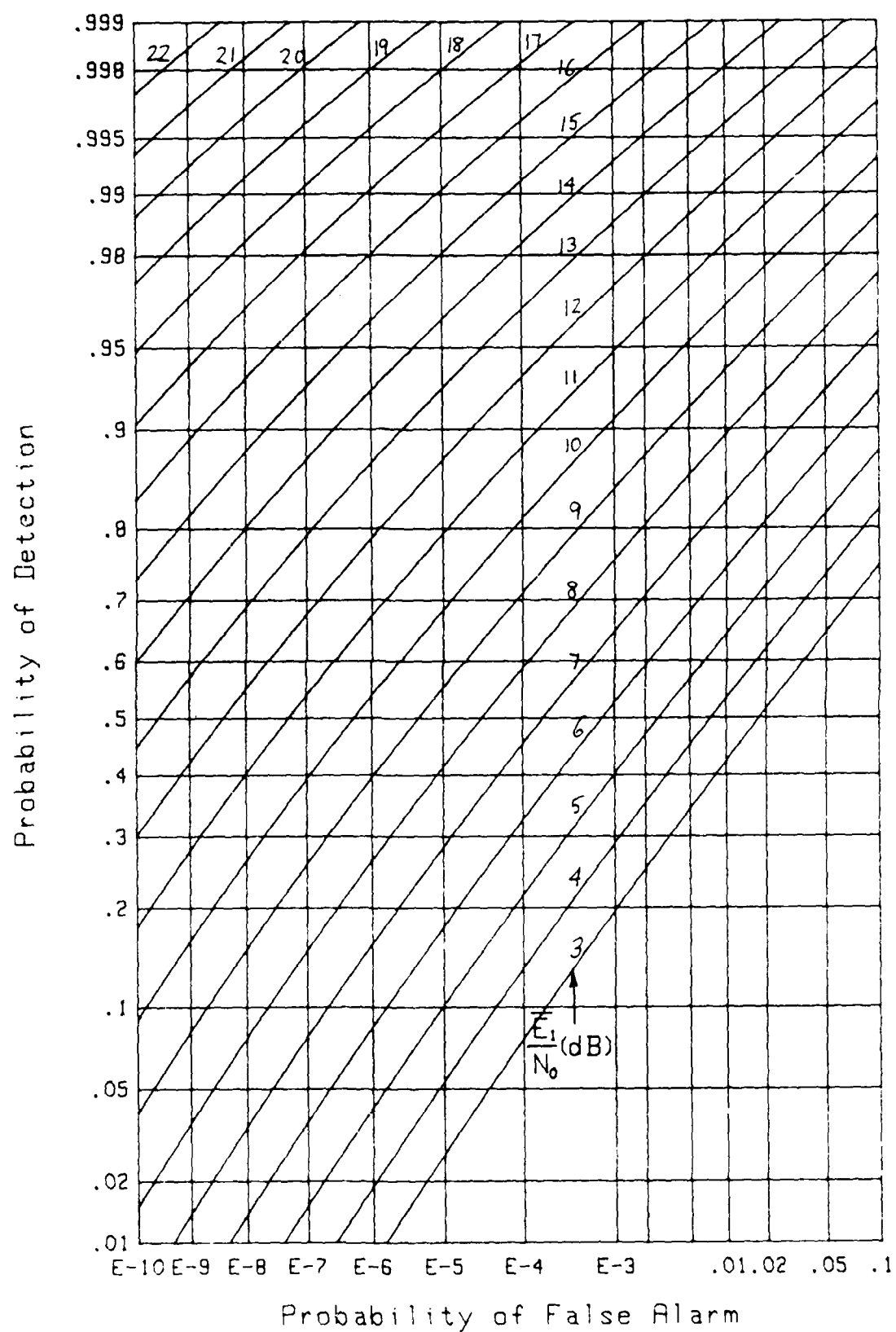
Figure 18. ROC for  $K=2$ ,  $m=.5$ ,  $\rho=.5$ ,  $L=32$

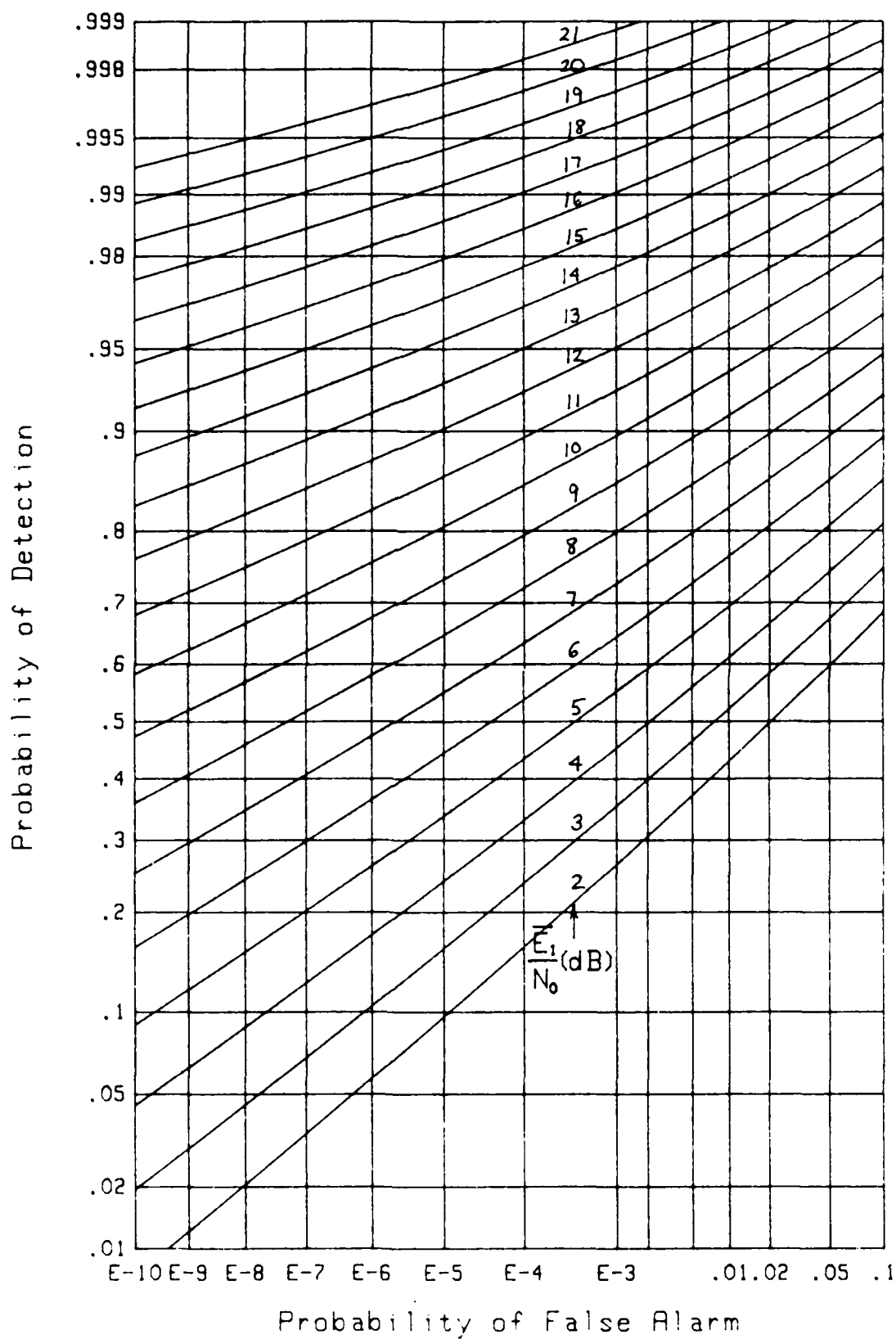
Figure 19. ROC for  $K=2$ ,  $m=.5$ ,  $\rho=.5$ ,  $L=16$

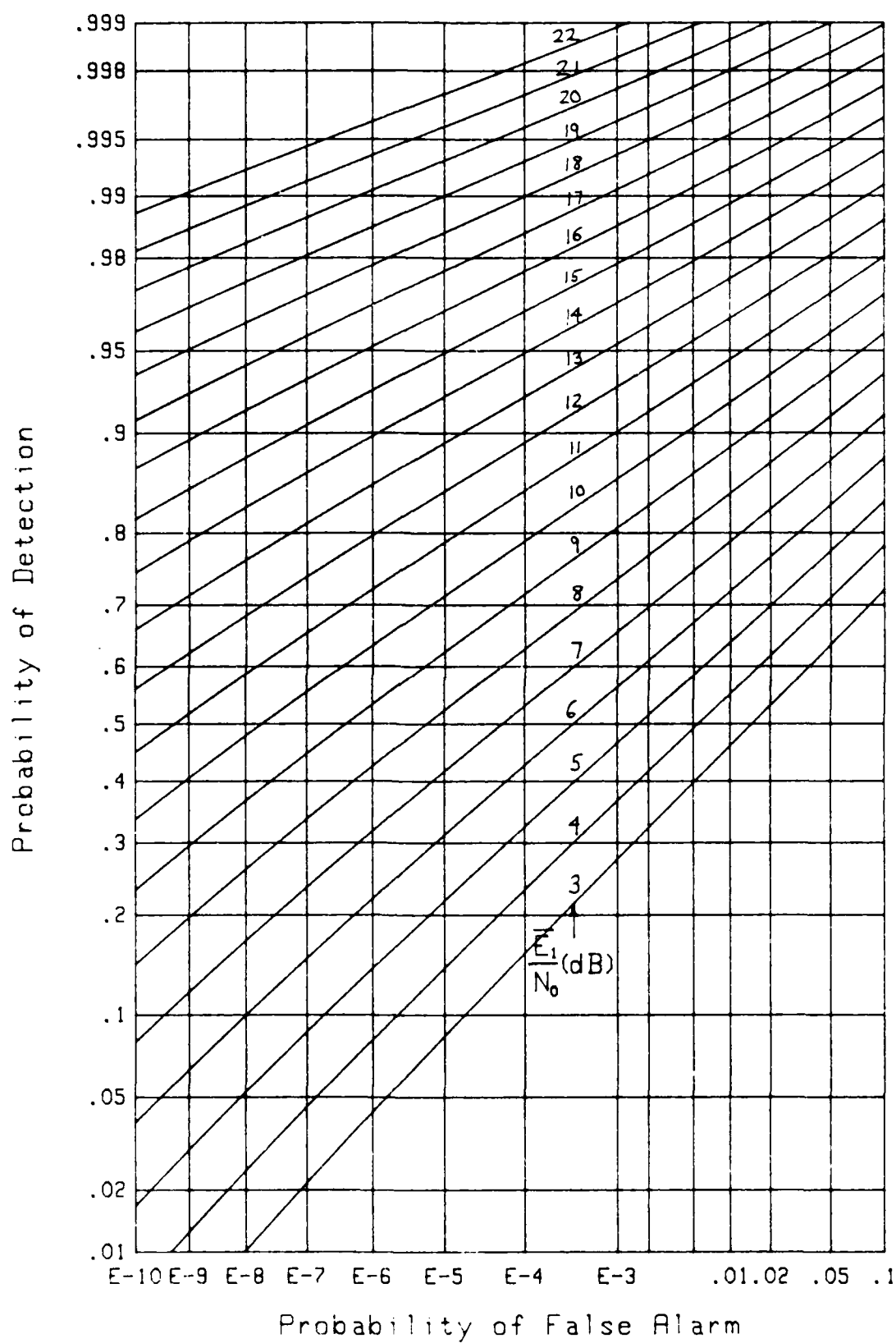


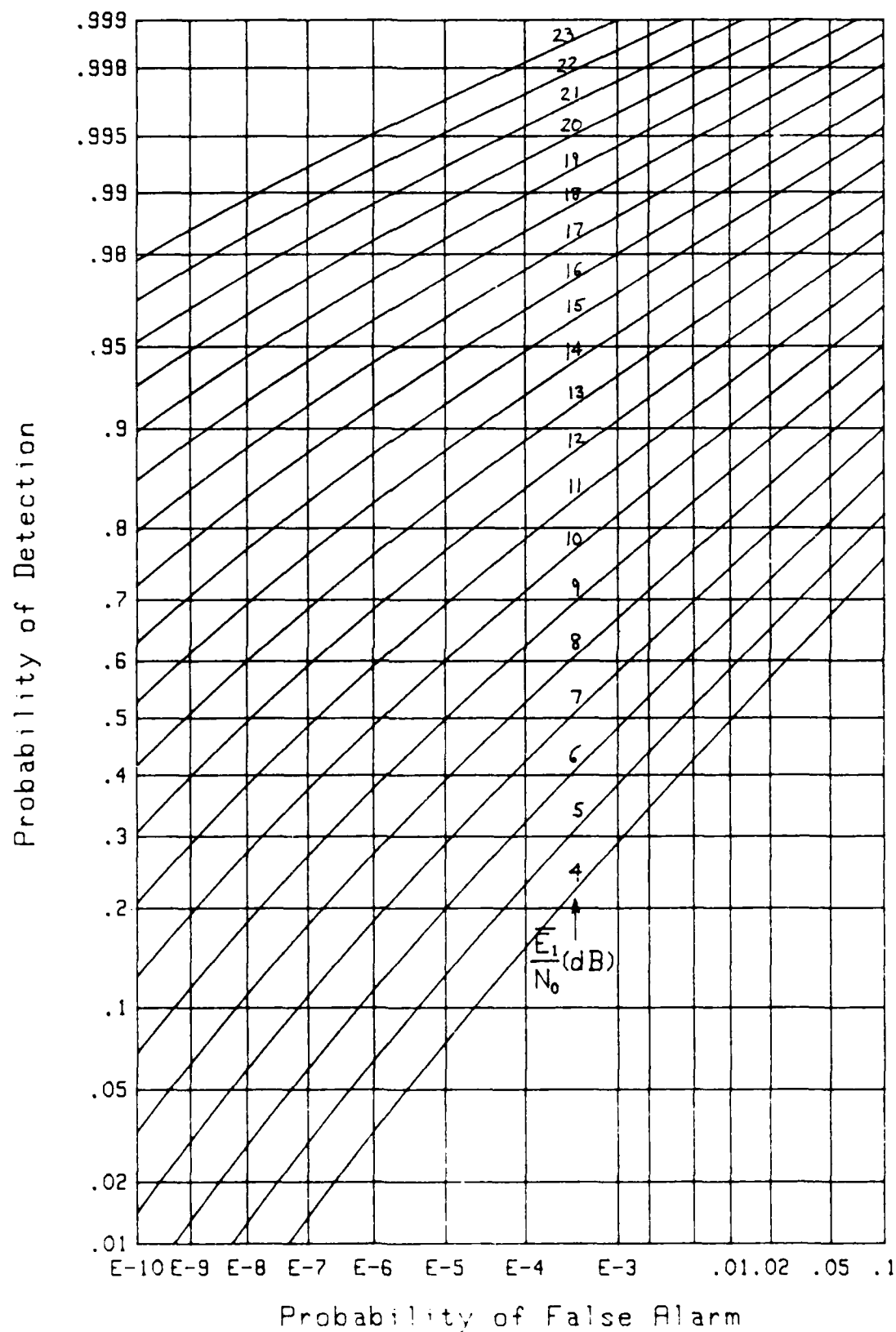
Figure 20. ROC for  $K=4$ ,  $m=1$ ,  $\rho=0$ ,  $L=\infty$

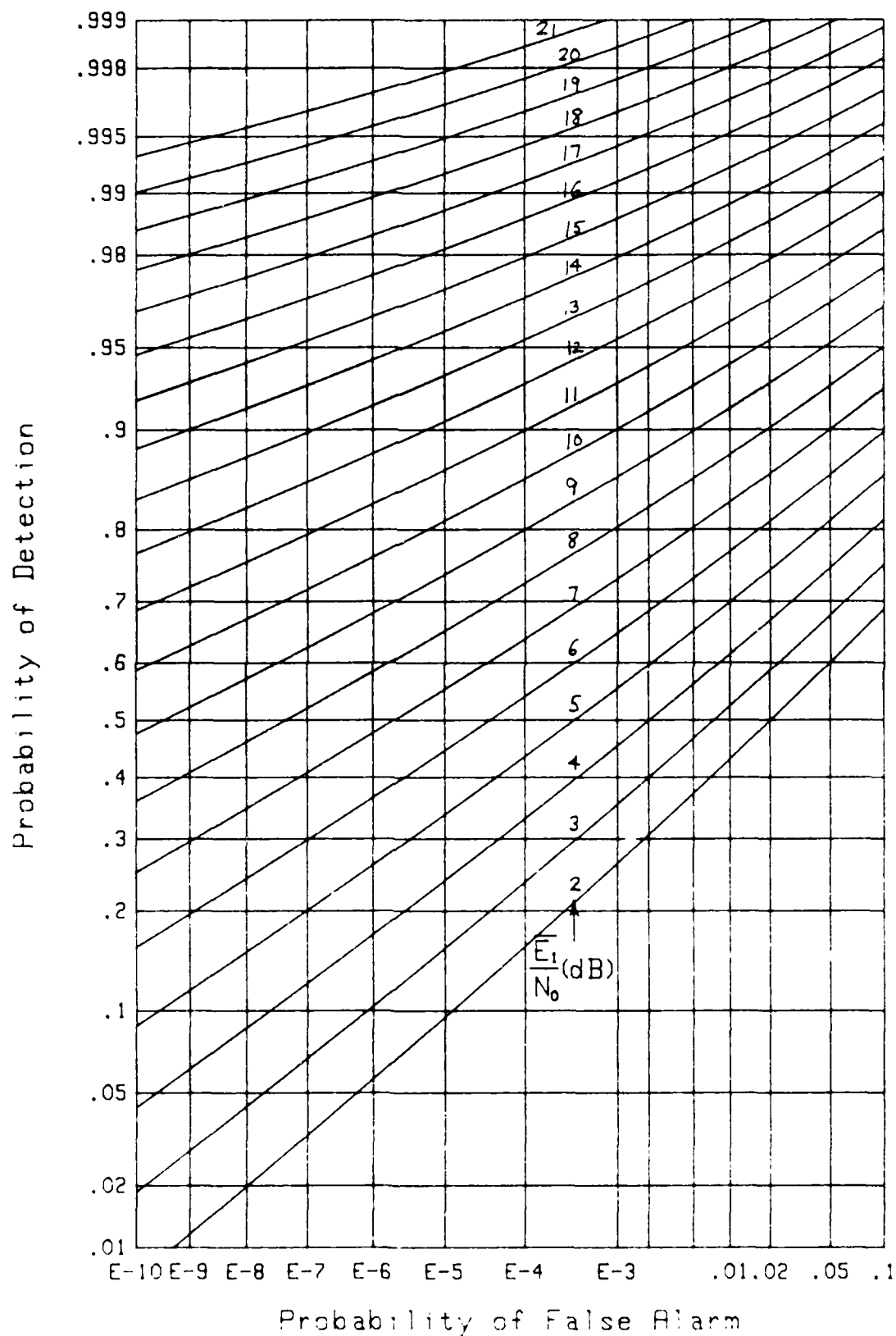


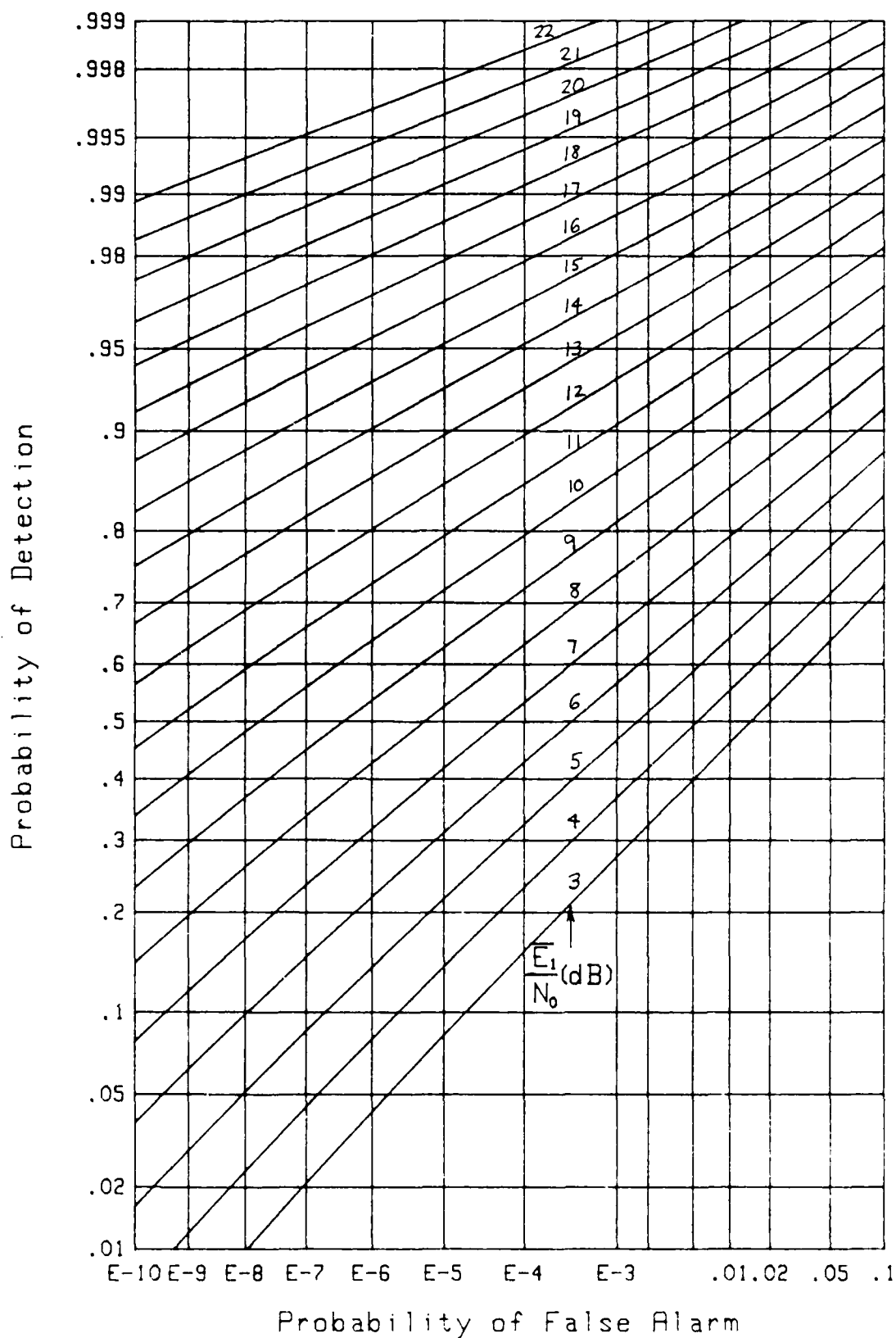
Figure 22. ROC for  $K=4$ ,  $m=1$ ,  $\rho=0$ ,  $L=16$

Figure 23. ROC for  $K=4$ ,  $m=1$ ,  $\rho=.5$ ,  $L=\infty$

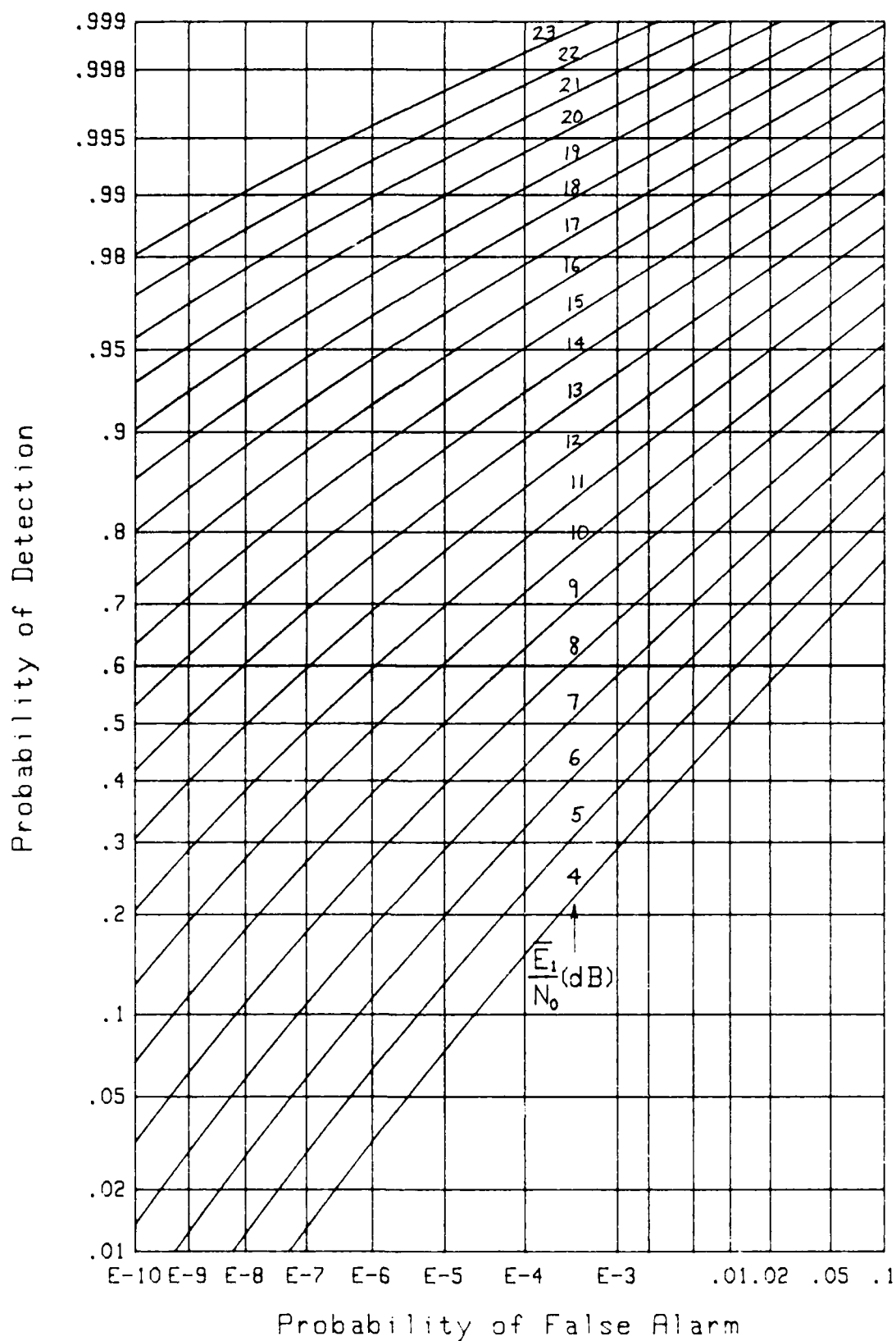
Figure 24. ROC for  $K=4$ ,  $m=1$ ,  $\rho=.5$ ,  $L=32$

Figure 25. ROC for  $K=4$ ,  $m=1$ ,  $\rho=.5$ ,  $L=16$

Figure 26. ROC for  $K=4$ ,  $m=.5$ ,  $\rho=0$ ,  $L=\infty$

Figure 27. ROC for  $K=4$ ,  $m=.5$ ,  $\rho=0$ ,  $L=32$



Figure 28. ROC for  $K=4$ ,  $m=.5$ ,  $\rho=0$ ,  $L=16$

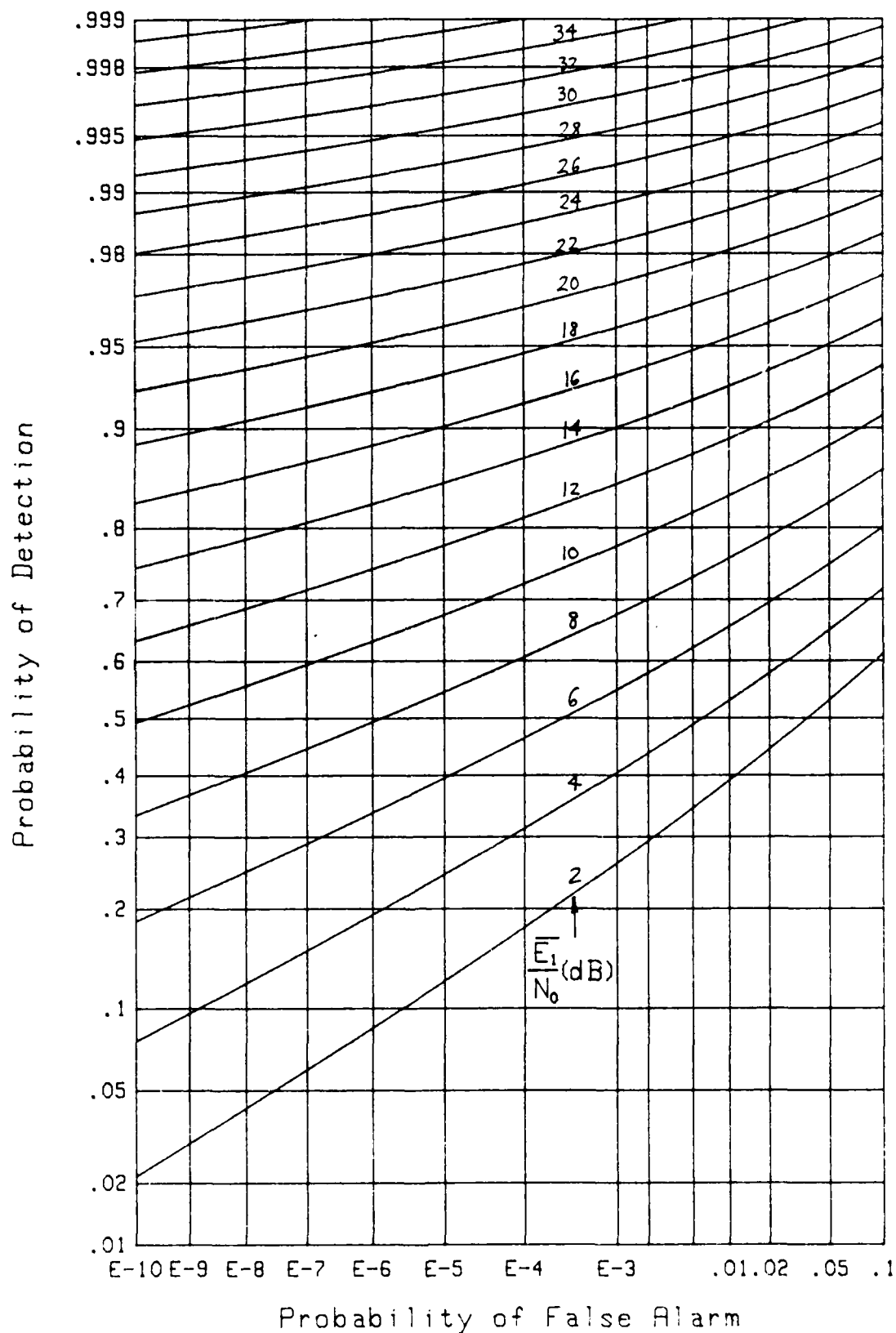
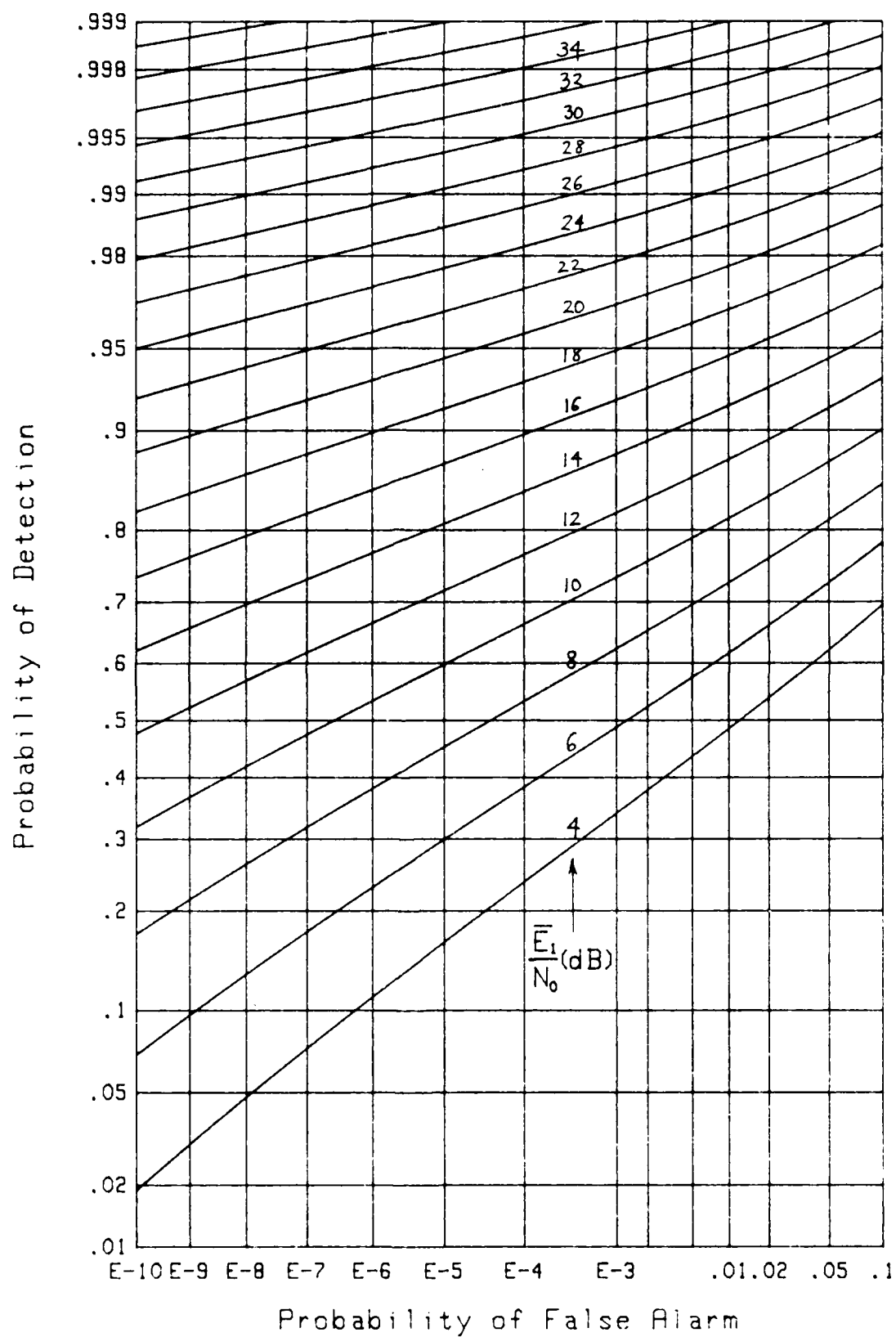
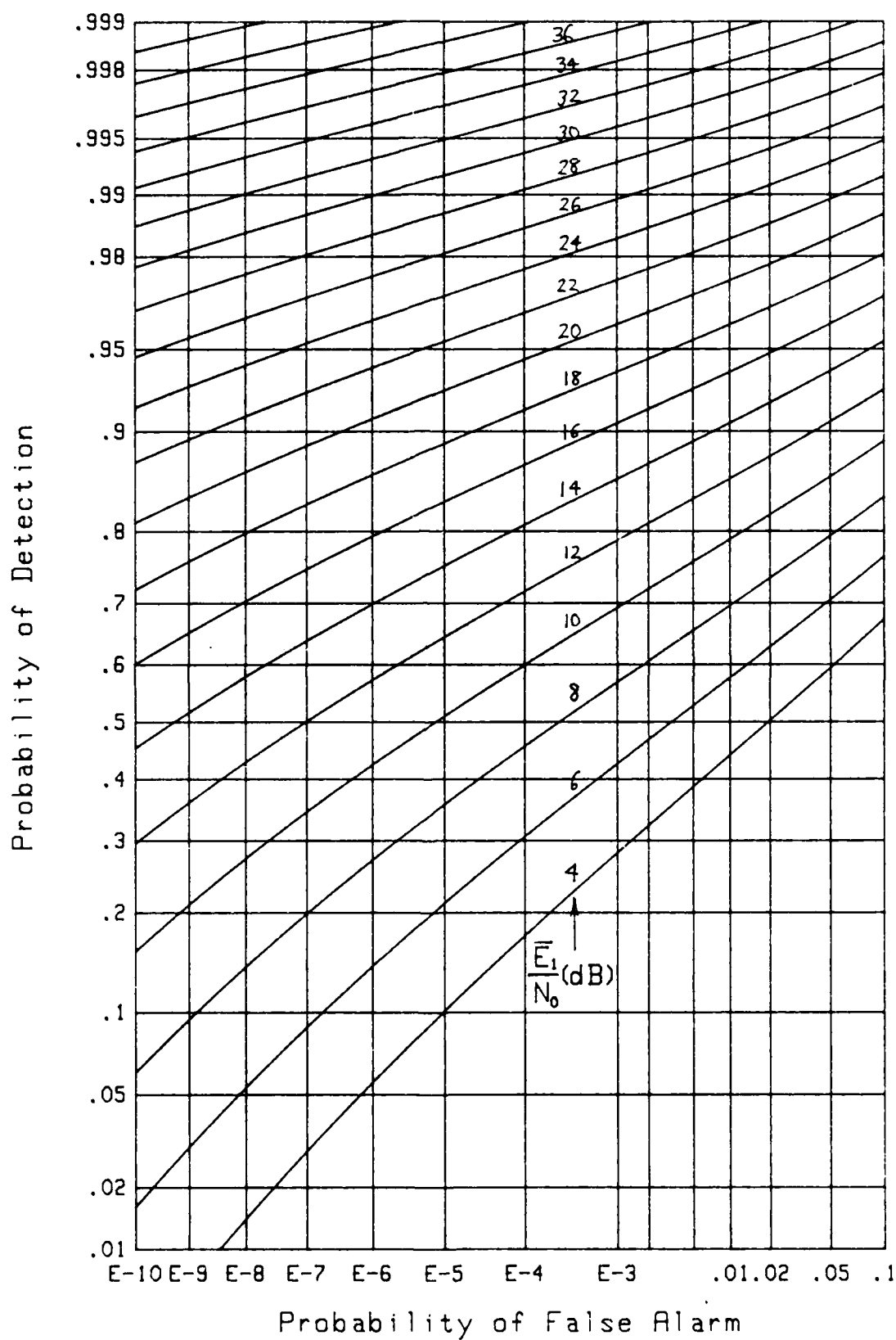
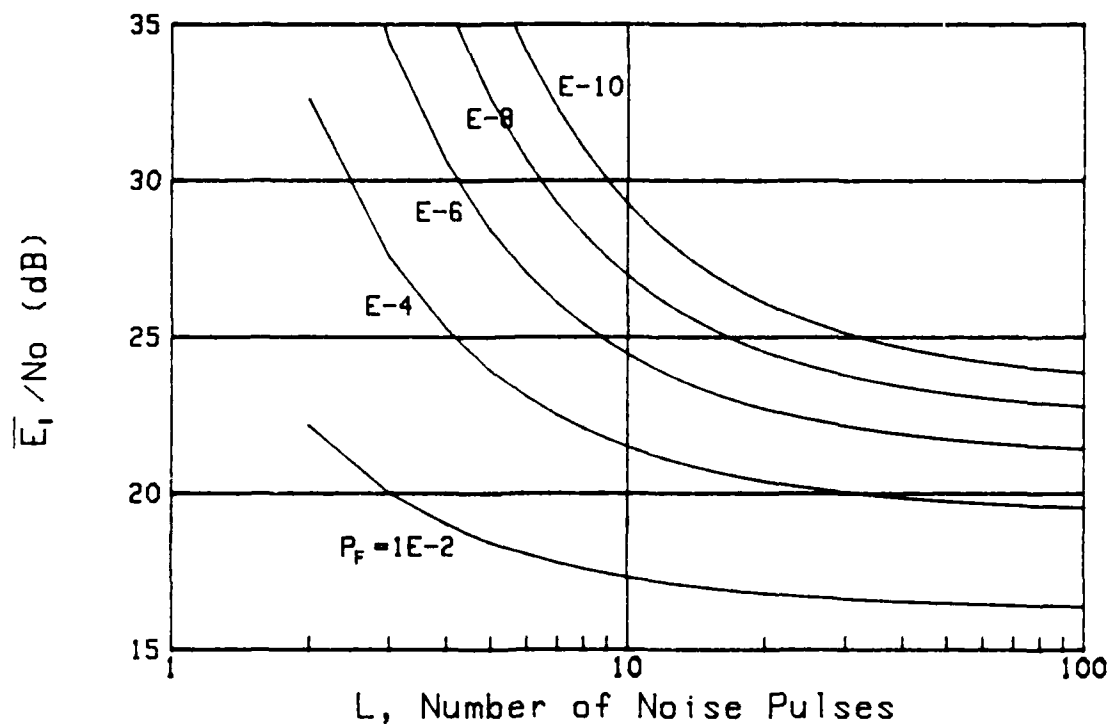
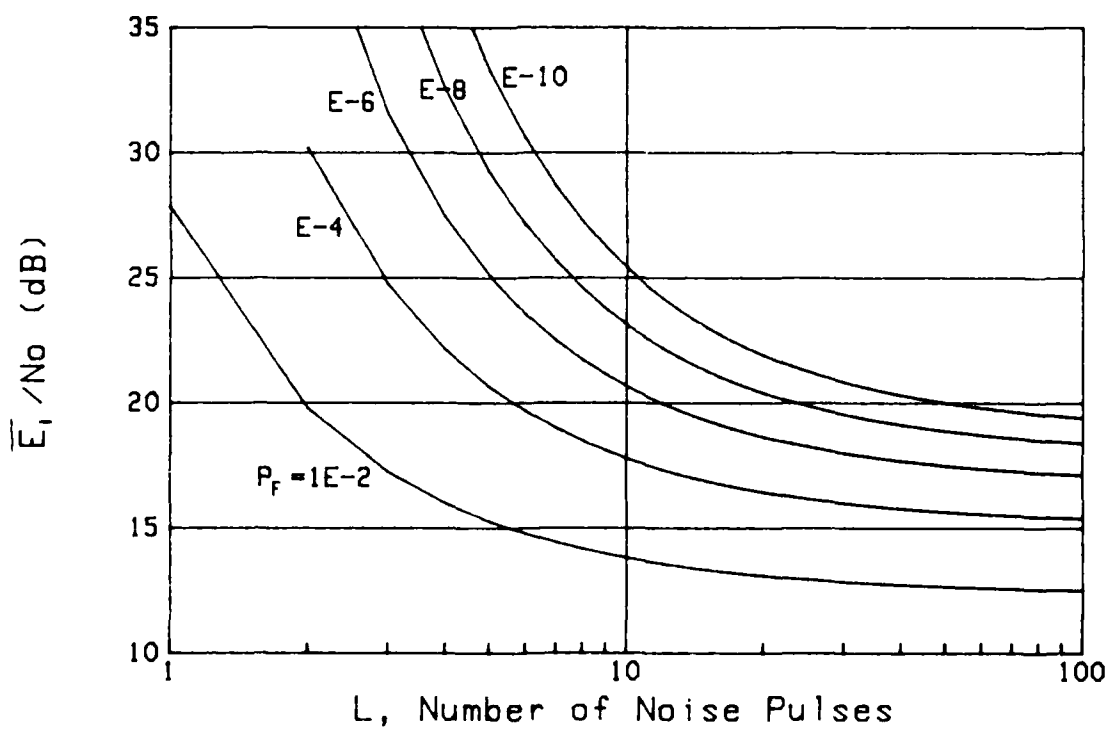


Figure 29. ROC for  $K=4$ ,  $m=.5$ ,  $\rho=.5$ ,  $L=\infty$

Figure 30. ROC for  $K=4$ ,  $m=.5$ ,  $\rho=.5$ ,  $L=32$

Figure 31. ROC for  $K=4$ ,  $m=.5$ ,  $\rho=.5$ ,  $L=16$

Figure 32. SNR for  $P_D = .9$ ,  $K=1$ ,  $m=1$ Figure 33. SNR for  $P_D = .9$ ,  $K=2$ ,  $m=1$ ,  $\rho = .5$

APPENDIX A  
PROGRAM LISTINGS

There are two programs listed in this appendix, the first for  $L$  finite, the second for  $L$  infinite, where  $L$  is the number of noise-only pulses used to establish a reference. The fundamental parameters  $K, m, L$  are input in lines 20, 30, 40, while  $\rho$  is input in line 1400. The particular values of  $\bar{E}_1/N_0$  (in dB) that are of interest are input in lines 340 and 350. Provision is made for 20  $P_D$  vs  $P_F$  curves in lines 60-90; this can easily be changed to accommodate other cases.

The false alarm and detection probabilities are available in lines 1000 and 1130, respectively. The detection probability utilizes  $R$  and  $N$  as input variables; see table 2. The particular covariance programmed in lines 1390-1430 is exponential, but this, too, can easily be generalized.

To save space, the complete program for  $L$  infinite is not listed. Rather, just the essential false alarm and detection probability routines are listed at the end of the appendix; these are obviously not functions of  $L$ . The changes required to accommodate this case of infinite  $L$  should be obvious.

```

10  ' GENERATE PD-VS-PF NUMBERS FOR FINITE L
20  K=4                ' NUMBER OF SIGNAL PULSES ADDED, K
30  Ms=.5              ' FADING PARAMETER, m (2m DOF)
40  L=16              ' NUMBER OF NOISE PULSES ADDED L
50  DIM U(100)
60  COM Pf(100),Pd1(100),Pd2(100),Pd3(100),Pd4(100),Pd5(100)
70  COM Pd6(100),Pd7(100),Pd8(100),Pd9(100),Pd10(100),Pd11(100)
80  COM Pd12(100),Pd13(100),Pd14(100),Pd15(100),Pd16(100),Pd17(100)
90  COM Pd18(100),Pd19(100),Pd20(100)
100 DOUBLE K,L,I,J    ' INTEGERS
110 S=0.
120 FOR I=1 TO K
130   FOR J=1 TO K
140    S=S+FNCOv(I,J)  ' NORMALIZED COVARIANCE COEFFICIENTS
150   NEXT J
160  NEXT I
170  Ke=K*K/5          ' EQUIVALENT NUMBER OF INDEPENDENT FADES
180  N=Ms*Ke           ' N = m Ke
190  U=0.
200  U=U+.01
210  Pf=FNPf(U,K,L)
220  IF Pf>.1 THEN 200
230  U1=MAX(U-.01,.01)
240  U=U+.01
250  Pf=FNPf(U,K,L)
260  IF Pf>1E-10 THEN 240
270  U2=U
280  Delu=(U2-U1)/100.
290  FOR I=0 TO 100
300   U=U1+Delu*I
310   U(I)=U           ' THRESHOLD VALUES
320   Pf(I)=FNPf(U,K,L) ' PROBABILITY OF FALSE ALARM
330  NEXT I
340  FOR J=1 TO 20
350   E1nodb=2+J+2      ' SIGNAL-TO-NOISE RATIO PER PULSE, E1/N0 (dB)
360   E1no=10.**.1*E1nodb
370   R=E1no*K/N
380   FOR I=0 TO 100
390    U=U(I)
400    Pd=FNPd(U,R,N,K,L) ' PROBABILITY OF DETECTION
410    IF J=1 THEN Pd1(I)=Pd
420    IF J=2 THEN Pd2(I)=Pd
430    '
440    '
450    IF J=19 THEN Pd19(I)=Pd
460    IF J=20 THEN Pd20(I)=Pd
470  NEXT I
480  NEXT J
490  FOR I=0 TO 100
500   Pf(I)=FNInophf(Pf(I))
510   Pd1(I)=FNInophf(Pd1(I))
520   Pd2(I)=FNInophf(Pd2(I))
530   '
540   '
550   Pd19(I)=FNInophf(Pd19(I))
560   Pd20(I)=FNInophf(Pd20(I))
570  NEXT I
580  CALL A
590  END
600  '

```

```

890 DEF FNInphi(X) ! AMS 55, 26.2.23
900 IF X=.5 THEN RETURN 0.
910 P=MIN(X,1.-X)
920 T=-LOG(P)
930 T=SQR(T+T)
940 P=1.+T*+.1432788+T*+.189269+T*+.001308+
950 P=T*(2.515517+T*+.002853+T*+.010328)/P
960 IF X<.5 THEN P=-P
970 RETURN P
980 FNEND
990 !
1000 DEF FNPd(U,DOUBLE K,L) ! FALSE ALARM PROBABILITY
1010 IF U<=0. THEN RETURN 1.
1020 DOUBLE Ls ! INTEGER
1030 U1=U+1.
1040 K1=K-1
1050 S=T=EXP(K*LOG(U/U1))
1060 FOR Ls=1 TO L-1
1070 T=T*(K1+Ls)/(Ls*U1)
1080 S=S+T
1090 NEXT Ls
1100 RETURN 1.-S
1110 FNEND
1120 !
1130 DEF FNPd(U,R,N,DOUBLE K,L) ! DETECTION PROBABILITY
1140 IF U<=0. THEN RETURN 1.
1150 DOUBLE Ls ! INTEGER
1160 U1=U+1.
1170 R1=R+1.
1180 U2=U/U1
1190 Ru=R1+U
1200 K2=K-2
1210 Nk=N-K+1
1220 Y=R1/Ru
1230 X=U2*R/R1
1240 X1=X-1.
1250 S=T=EXP(K*LOG(U2)+N*LOG(U1-Ru))
1260 Ho=0.
1270 H=1.
1280 FOR Ls=1 TO L-1
1290 T=T*Y
1300 J=K2+Ls
1310 A=((J+Ls+(N-Ls)*X)+H+J*X1+Ho)/Ls
1320 Ho=H
1330 H=A
1340 S=S+T*H
1350 NEXT Ls
1360 RETURN 1.-S
1370 FNEND
1380 !
1390 DEF FNCov(DOUBLE I,J)
1400 Rho=.5 ! NORMALIZED COVARIANCE COEFFICIENT
1410 Cov=Rho*ABS(I-J) ! EXPONENTIAL BEHAVIOR
1420 RETURN Cov
1430 FNEND
1440 !

```



```

1450 SUB R      ! PLOT PD VS PF ON NORMAL PROBABILITY PAPER
1460 COM PF(*),Pd1(*),Pd2(*),Pd3(*),Pd4(*),Pd5(*)
1470 COM Pd6(*),Pd7(*),Pd8(*),Pd9(*),Pd10(*),Pd11(*)
1480 COM Pd12(*),Pd13(*),Pd14(*),Pd15(*),Pd16(*),Pd17(*)
1490 COM Pd18(*),Pd19(*),Pd20(*)
1500 DIM A$(30),B$(30)
1510 DIM Xlabel$(1:30),Ylabel$(1:30)
1520 DIM Xcoord(1:30),Ycoord(1:30)
1530 DIM Xgrid(1:30),Ygrid(1:30)
1540 DOUBLE N,Lx,Ly,Nx,Ny,I      ! INTEGERS
1550 !
1560 A$="Probability of False Alarm"
1570 B$="Probability of Detection"
1580 !
1590 Lx=12
1600 REDIM Xlabel$(1:Lx),Xcoord(1:Lx)
1610 DATA E-10,E-9,E-8,E-7,E-6,E-5,E-4,E-3,.01,.02,.05,.1
1620 READ Xlabel$(*)
1630 DATA 1E-10,1E-9,1E-8,1E-7,1E-6,1E-5,1E-4,.001,.01,.02,.05,.1
1640 READ Xcoord(*)
1650 !
1660 Ly=18
1670 REDIM Ylabel$(1:Ly),Ycoord(1:Ly)
1680 DATA .01,.02,.05,.1,.2,.3,.4,.5,.6,.7,.8,.9
1690 DATA .95,.98,.99,.995,.998,.999
1700 READ Ylabel$(*)
1710 DATA .01,.02,.05,.1,.2,.3,.4,.5,.6,.7,.8,.9
1720 DATA .95,.98,.99,.995,.998,.999
1730 READ Ycoord(*)
1740 !
1750 Nx=14
1760 REDIM Xgrid(1:Nx)
1770 DATA 1E-10,1E-9,1E-8,1E-7,1E-6,1E-5,1E-4
1780 DATA .001,.002,.005,.01,.02,.05,.1
1790 READ Xgrid(*)
1800 !
1810 Ny=18
1820 REDIM Ygrid(1:Ny)
1830 DATA .01,.02,.05,.1,.2,.3,.4,.5,.6,.7,.8,.9
1840 DATA .95,.98,.99,.995,.998,.999
1850 READ Ygrid(*)
1860 !
1870 FOR I=1 TO Lx
1880 Xcoord(I)=FNInuphi(Xcoord(I))
1890 NEXT I
1900 FOR I=1 TO Ly
1910 Ycoord(I)=FNInuphi(Ycoord(I))
1920 NEXT I
1930 FOR I=1 TO Nx
1940 Xgrid(I)=FNInuphi(Xgrid(I))
1950 NEXT I
1960 FOR I=1 TO Ny
1970 Ygrid(I)=FNInuphi(Ygrid(I))
1980 NEXT I
1990 X1=Xgrid(1)
2000 X2=Xgrid(Nx)
2010 Y1=Ygrid(1)
2020 Y2=Ygrid(Ny)
2030 Scale=(Y2-Y1)/(X2-X1)

```

```

2040 GINIT 200., 260.
2050 PLOTTER IS 505, "HPGL"
2060 PRINTER IS 505
2070 PRINT "VS4"
2080 LIMIT PLOTTER 505, 0., 200., 0., 260.
2090 VIEWPORT 22., 85., 19., 122.
2100 VIEWPORT 22., 85., 59., 122.
2110 VIEWPORT 22., 85., 19., 62.
2120 WINDOW X1, X2, Y1, Y2
2130 FOR I=1 TO Nx
2140 MOVE Xgrid(I), Y1
2150 DRAW Xgrid(I), Y2
2160 NEXT I
2170 FOR I=1 TO Ny
2180 MOVE X1, Ygrid(I)
2190 DRAW X2, Ygrid(I)
2200 NEXT I
2210 CSIZE 2.3, .5
2220 LORG 5
2230 Y=Y1-(Y2-Y1)*.02
2240 FOR I=1 TO Lx
2250 MOVE Xcoord(I), Y
2260 LABEL Xlabel$(I)
2270 NEXT I
2280 CSIZE 3., .5
2290 MOVE .5*(X1+X2), Y1-.06*(Y2-Y1)
2300 LABEL A$
2310 MOVE .5*(X1+X2), Y1-.1*(Y2-Y1)
2320 LABEL "Figure 31. ROC for K=4, m=.5, n=.5, L=16"
2330 CSIZE 2.3, .5
2340 LORG 8
2350 X=X1-(X2-X1)*.01
2360 FOR I=1 TO Ly
2370 MOVE X, Ycoord(I)
2380 LABEL Ylabel$(I)
2390 NEXT I
2400 LDIR PI 2.
2410 CSIZE 3., .5
2420 LORG 5
2430 MOVE X1-.15*(X2-X1), .5*(Y1+Y2)
2440 LABEL B$
2450 PENUP
2460 PLOT Pf(*), Pd1(*)
2470 PENUP
2480 PLOT Pf(*), Pd2(*)
2490 PENUP
2500
2510
2520 PLOT Pf(*), Pd19(*)
2530 PENUP
2540 PLOT Pf(*), Pd20(*)
2550 PENUP
2560 PAUSE
2570 PRINTER IS CRT
2580 PLOTTER 505 IS TERMINATED
2590 SUBEND

```

```

10  DEF FNPF(Thr,DOUBLE E)  FALSE ALARM PROBABILITY
20  DOUBLE J
30  S=T=EXP(-Thr)
40  FOR J=1 TO K-1
50  T=T*Thr/J
60  S=S+T
70  NEXT J
80  RETURN S
90  FNEND
100
110  DEF FNPD(Thr,R,N,DOUBLE E)  TR 7707, APP. C-1
120  Error=1.E-10
130  DOUBLE K1,Ks
140  Et=EXP(Thr)
150  K1=K-1
160  N1=N-1.
170  R1=1.+R
180  Q=R/R1
190  E=Te=1.
200  FOR Ks=1 TO K1
210  Te=Te*Thr/Ks
220  E=E+Te
230  NEXT Ks
240  S=B=MAX(Et-E,0.)
250  T=1.
260  FOR Ks=1 TO 1000
270  Te=Te*Thr/(K1+Ks)
280  B=MAX(B-Te,0.)
290  T=T+Q*(N1+Ks)/Ks
300  Pr=T*B
310  S=S+Pr
320  IF ABS(Pr) =Error*ABS(S) THEN 350
330  NEXT Ks
340  PRINT "1000 TERMS AT: ";K;N;Thr;R;Pr;S
350  Pd=1.-EXP(-Thr-N*LOG(R100)*S
360  RETURN Pd
370  FNEND

```

## REFERENCES

1. A. H. Nuttall and E. S. Eby, Signal-to-Noise Ratio Requirements for Detection of Multiple Pulses Subject to Partially Correlated Fading With Chi-Squared Statistics of Various Degrees of Freedom, NUSC Technical Report 7707, Naval Underwater Systems Center, New London, CT, 2 June 1986.
2. Handbook of Mathematical Functions, U. S. Department of Commerce, National Bureau of Standards, Applied Mathematics Series No. 55, U. S. Government Printing Office, Washington, D.C., June 1964.
3. I. S. Gradshteyn and I. M. Ryzhik, Table of Integrals, Series, and Products, Academic Press, Inc., New York, NY, 1980.
4. A. H. Nuttall and P. G. Cable, Operating Characteristics for Maximum Likelihood Detection of Signals in Gaussian Noise of Unknown Level: III. Random Signals of Unknown Level, NUSC Technical Report 4783, Naval Underwater Systems Center, New London, CT, 31 July 1974.
5. D. R. Morgan, "Two-Dimensional Normalization Techniques," IEEE Journal of Oceanic Engineering, vol. OE-12, no. 1, pp. 130-142, January 1987.
6. A. H. Nuttall, Operating Characteristics of Log-Normalizer for Weibull and Log-Normal Inputs, NUSC Technical Report 8075, Naval Underwater Systems Center, New London, CT, 17 August 1987.
7. A. H. Nuttall, Operating Characteristics for Indicator Or-ing of Incoherently Combined Matched-Filter Outputs, NUSC Technical Report 8121, Naval Underwater Systems Center, New London, CT, 21 September 1987.

## INITIAL DISTRIBUTION LIST

Addressee	No. of Copies
ADMIRALTY UNDERWATER WEAPONS ESTAB., DORSET, ENGLAND	1
ADMIRALTY RESEARCH ESTABLISHMENT, LONDON, ENGLAND (Dr. L. Lloyd)	1
APPLIED PHYSICS LAB, JOHN HOPKINS	1
APPLIED PHYSICS LAB, U. WASHINGTON	1
APPLIED RESEARCH LAB, PENN STATE	1
APPLIED RESEARCH LAB, U. TEXAS	1
APPLIED SEISMIC GROUP, CAMBRIDGE, MA (R. Lacoss)	1
A & T, STONINGTON, CT (H. Jarvis)	1
APPLIED SEISMIC GROUP, (R. Lacoss)	1
ASTRON RESEARCH & ENGR, SANTA MONICA, CA (Dr. A. Piersol)	1
ASW SIGNAL PROCESSING, MARTIN MARIETTA BALTIMORE AEROSPACE (S. L. Marple)	1
AUSTRALIAN NATIONAL UNIV. CANBERRA, AUSTRALIA (Prof. B. Anderson)	1
BBN, Arlington, Va. (Dr. H. Cox)	1
BBN, Cambridge, MA (H. Gish)	1
BBN, New London, Ct. (Dr. P. Cable)	1
BELL COMMUNICATIONS RESEARCH, Morristown, NJ (J. Kaiser)	1
BENDAT, JULIUS DR., 833 Moraga Dr., LA, CA	1
BROWN UNIV., PROVIDENCE, RI (Documents Library)	1
CANBERRA COLLEGE OF ADV. EDUC, BELCONNEN, A.C.T. AUSTRALIA (P. Morgan)	1
COAST GUARD ACADEMY, New London, CT (Prof. J. Wolcin)	1
COAST GUARD R & D, Groton, CT (Library)	1
COGENT SYSTEMS, INC, (J. Costas)	1
COLUMBIA RESEARCH CORP, Arlington, VA 22202 (W. Hahn)	1
CONCORDIA UNIVERSITY H-915-3, MONTREAL, QUEBEC CANADA (Prof. Jeffrey Krolik)	1
CNO, Wash, DC	1
DAVID W. TAYLOR NAVAL SHIP R&D CNTR, BETHESDA, MD	1
DARPA, ARLINGTON, VA (A. Ellinthorpe)	1
DALHOUSIE UNIV., HALIFAX, NOVA SCOTIA, CANADA (Dr. B. Ruddick)	1
DEFENCE RESEARCH ESTAB. ATLANTIC, DARTMOUTH, NOVA SCOTIA (Library)	1
DEFENCE RESEARCH ESTAB. PACIFIC, VICTORIA, CANADA (Dr. D. Thomson)	1
DEFENCE SCIENTIFIC ESTABLISHMENT, MINISTRY OF DEFENCE, AUCKLAND, N Z. (Dr. L. Hall)	1
DEFENCE RESEARCH CENTRE, ADELAIDE, AUSTRALIA	1
DEFENSE SYSTEMS, INC, MC LEAN, VA (Dr. G. Sebestyen)	1
DTNSROC	1
DTIC	2
DREXEL UNIV, (Prof. S. Kesler)	1
Dr. Julius Bendat, 833 Moraga Drive, Los Angeles, CA	1
ECOLE ROYALE MILITAIRE, BRUXELLES, BELGIUM (Capt J. Pajot)	1
EDO CORP, College Point, NY	1
EG&G, Manassas, VA (Dr. J. Huguen)	1
ENGINEERING SOCIETIES LIBRARY, NY, NY	1
FUNK, DALE, Seattle, Wn	1

GENERAL ELECTRIC CO. PITTSFIELD, MA (Mr. J. Rogers)	1
GENERAL ELECTRIC CO, SYRACUSE, NY (Mr. R. Race)	1
HAHN, WM, Apt. 701, 500 23rd St. NW, Wash, DC 20037	1
HARRIS SCIENTIFIC SERVICES, Dobbs Ferry, NY (B. Harris)	1
HARVARD UNIV, CAMBRIDGE, MA (Library)	1
HONEYWELL, INC., Seattle, WN (D. Goodfellow)	1
HUGHES AIRCRAFT, Fullerton, CA (S. Autrey)	1
IBM, Manassas, VA (G. Demuth)	1
INDIAN INSTITUTE OF SCIENCE, BANGALORE, INDIA (N. Srinivasa)	1
JOHNS HOPKINS UNIV, LAUREL, MD (J. C. Stapleton)	1
M/A-COM, BURLINGTON, MA (Dr. R. Price)	1
MAGNAVOX GOV & IND ELEC CO, Ft. Wayne, IN (R. Kenefic)	1
MARINE BIOLOGICAL LAB, Woods Hole, MA	1
MASS INSTITUTE OF TECH, Cambridge, MA (Library and (Prof. A. Baggaroer)	2
MAXWELL AIR FORCE BASE, ALABAMA (Library)	1
MBS SYSTEMS, NORWALK, CT (A. Winder)	1
MIDDLETON, DAVID, 127 E. 91st ST, NY, NY	1
MIKHALEVSKY, PETER, SAIC, 803 W. Broad St., Falls Church, VA.	1
NADC	1
NASC, NAIR-03	1
NATIONAL RADIO ASTRONOMY OBSERVATORY (F. Schwab)	1
NATO SACLANT ASW RESEARCH CNTR, APO, NY, NY (Library, E. J. Sullivan and G. Tacconi)	3
NAVAL INTELLIGENCE COMMAND	1
NAVAL INTELLIGENCE SUPPORT CTR	3
NAVAL OCEANOGRAPHY COMMAND	1
NAVAL OCEANOGRAPHIC OFFICE	1
NAVAL POSTGRADUATE SCHOOL, MONTEREY, CA (C. W. Therrien)	1
NAVAL RESEARCH LAB, Orlando, FL	1
NAVAL RESEARCH LAB, Washington, DC (Dr. P. B. Abraham; W. Gabriel, Code 5372; A Gerlach; and N. Yen (Code 5135)	4
NAVAL SYSTEMS DIV., SIMRAD SUBSEA A/S, NORWAY (E. B. Lunde)	1
NCEL	1
NCSC	1
NICHOLS RESEARCH CORP., Wakefield, MA (T. Marzetta)	1
NOP-098	1
NORDA (R. Wagstaff)	1
NORTHEASTERN UNIV. (Prof. C. L. Nikias)	1
NOSC, (F. J. Harris)	1
NPRDC	1
NPS	3
NRL, Washington, DC (Dr. P. Abraham, W. Gabriel, A. Gerlach and Dr. Yen)	4
NRL, UND SOUND REF DET, ORLANDO	1
NSWC	1
NSWC DET FT. LAUDERDALE	1
NSWC WHITE OAK LAB	1
NUSC DET FT. LAUDERDALE	1
NUSC DET TUDOR HILL	1
NUSC DET WEST PALM BEACH (Dr. R. Kennedy Code 3802)	1
NWC	1
OCNR-00, -10, -11, -12, -13, -20(2), -122, -123-, -124	10
OFFICE OF NAVAL RESEARCH, Arlington, VA (N. Gerr, Code 411)	1
ORI CO, INC, New London, CT (G. Assard)	1

PENN STATE UNIV., State College, PA (F. Symons)	1
PDW-124	1
PMS-409, -411	2
PROMETHEUS, INC, Sharon, MA (Dr. J. Byrnes)	1
PSI MARINE SCIENCES, New London, Ct. (Dr. R. Mellen)	1
RAN RESEARCH LAB, DARLINGHURST, AUSTRALIA	1
RAYTHEON CO, Portsmouth, RI (J. Bartram)	1
ROCKWELL INTERNATIONAL CORP. Anaheim, CA (L. Einstein and Dr. D. Elliott)	2
ROYAL MILITARY COLLEGE OF CANADA, (Prof. Y. Chan)	1
RCA CORP, Moorestown, NJ (H. Upkowitz)	1
SAIC, Falls Church, VA (Dr. P. Mikhalevsky)	1
SAIC, New London, CT (Dr. F. Dinapoli)	1
SANDIA NATIONAL LABORATORY (J. Claasen)	1
SCRIPPS INSTITUTION OF OCEANOGRAPHY	1
SEA-63, -63D,	2
SONAR & SURVEILLANCE GROUP, DARLINGHURST, AUSTRALIA	1
SOUTHEASTERN MASS. UNIV (Prof. C. H. Chen)	1
SPERRY CORP, GREAT NECK, NY	1
SPWAR-05	1
TEL-AVIV UNIV, TEL-AVIV, ISRAEL (Prof. E. Winstein)	1
TRACOR, INC, Austin, TX (Dr. T Leih and J. Wilkinson)	1
TRW FEDERAL SYSTEMS GROUP (R. Prager)	1
UNDERSEA ELECTRONICS PROGRAMS DEPT, SYRACUSE, NY (J. Rogers)	1
UNIV. OF ALBERTA, EDMONTON, ALBERTA, CANADA (K. Yeung)	1
UNIV OF CA, San Diego, CA (Prof. C. Helstrom)	1
UNIV OF CT, (Library and Prof. C. Knapp)	2
UNIV OF FLA, GAINESVILLE, FL (D. Childers)	1
UNIV OF MICHIGAN, Cooley Lab, Ann Arbor, MI (Prof T. Birdsall)	1
UNIV. OF MINN, Minneapolis, Mn (Prof. M. Kaveh)	1
UNIV. OF NEWCASTLE, NEWCASTLE, NSW, CANADA (Prof. A. Cantoni)	1
UNIV OF RI, Kingston, RI (Prof. S. Kay, Prof. L. Scharf, Prof. D. Tufts and Library)	4
UNIV. OF STRATHCLYDE, ROYAL COLLEGE, Glasgow, Scotland (Prof. T. Durrani)	1
UNIV. OF TECHNOLOGY, Loughborough, Leicestershire, England (Prof. J. Griffiths)	1
UNIV. OF WASHINGTON, Seattle (Prof. D. Lytle)	1
URICK, ROBERT, Silver Springs, MD	1
VAN ASSELT, HENRIK, USEA S.P.A., LA SPEZIA, ITALY	1
WEAPONS SYSTEM RESEARCH LAB, ADELAIDE, AUSTRALIA	2
WESTINGHOUSE ELEC. CORP, WALTHAM, MA (D. Bennett)	1
WESTINGHOUSE ELEC. CORP, OCEANIC DIV, ANNAPOLIS, MD (Dr. H. L. Price)	1
WINDER, A. Norwalk, CT	1
WOODS HOLE OCEANOGRAPHIC INSTITUTION (Dr. R. Spindel and Dr. E. Weinstein)	2
YALE UNIV. (Library and Prof. P. Schultheiss)	2

END

DATE

FILMD

3-88

DTIC